# MMF1928 Pricing Theory Project 4

## The Heston Model

by:

Manyi Luo (1003799419)

Spencer Sillaste (1008173851)

Yitian Zhang (1003838519)

December 2021

# Abstract

In this report, we investigated the Heston model and the impact of control variates to minimize the model variance. We first obtained the Euler discretization, Milstein discretization and mixing method for the continuous price process as well as the variance process scheme, which are used for doing Monte Carlo simulation of the implied volatility smiles with confidence intervals for both European style put and call options. It was found that the mixing method performed better than the Euler discretization method. Afterwards, we included control variates to the Heston model and derived the expressions of optimization parameter to minimize the model variance and the analytical expressions of various financial products used as control variates. These control variates were further compared by simulating the paths of the Heston model under deterministic volatility using Milstein discretization. The performance of control variates in the Euler discretization scheme was compared to the mixing method. It was found that using all the control variates for the Euler discretization method outperformed the mixing method.

# Contents


**1 Introduction** **1**

**2 Theoretical Framework** **2**

2.1 Fundamental Setting . . . . . 2

2.2 Implied Volatility . . . . . 2

2.3 Numerical Solutions to Stochastic Differential Equations . . . . . 3

2.3.1 Euler Method . . . . . 4

2.3.2 Milstein Method . . . . . 4

2.4 Heston Model . . . . . 5

2.4.1 Model setup . . . . . 5

2.4.2 Risk Neutral Dynamics . . . . . 6

2.5 Control Variate . . . . . 7

**3 Mathematical Derivations** **8**

3.1 Heston Model . . . . . 8

3.1.1 Euler Method . . . . . 8

3.1.2 Milstein Method . . . . . 10

3.1.3 Mixing Method . . . . . 12

3.1.4 An Example of Derivative Valuation . . . . . 12

3.2 Control Variate and the Optimal Choice of $\gamma_i$ . . . . . 15

3.3 Analytical Closed-form Expressions for Heston Model . . . . . 17

3.4 Value of a Contingent Claim . . . . . 20

3.4.1 Paying $\int_0^T v_s ds$ at maturity $T$ . . . . . 20

3.4.2 Paying $\int_0^T v_s^2 ds$ at maturity $T$ . . . . . 20

**4 Implementation, Results and Analysis** **22**

4.1 Implied Volatilities from Direct Numerical Solutions to the Heston Model . . 22

4.1.1 Discretization Approach . . . . . 24

4.1.2 Mixing Method . . . . . 28

4.2 Contingent Claim Valuation . . . . . 32
4.3 Implied Volatilities from Control Variate Simulations . . . . . 35

**5 Conclusion** **40**

**6 Appendix: Discretization and Mixing Methods** **41**

**7 Appendix: Control Variates** **43**

7.1 Claim Paying $\int_0^T v_s ds$ . . . . . 43
7.1.1 Heston Model . . . . . 43
7.1.2 Deterministic Volatility Model . . . . . 45

# 1 Introduction

In this report, we would like to investigate several aspects of the Heston model. Using the basic Heston model set up, we would like to estimate the implied volatility smiles with confidence intervals for both put and call options. Therefore, we conducted the Euler discretization, Milstein discretization, mixing method for the continuous price process as well as the variance process, and obtained the corresponding results using Monte Carlo simulation. Afterwards, we studied the impact of control variates to reduce the variance of a Monte Carlo simulation when having an analytic solution of a closely related model. We derived the expression of optimization parameter to minimize the model variance, and calculated various closed-form expressions for options to be used as control variates, including the price of the option and the value of two contingent claims. Additionally, we simulated paths of the Heston model under the deterministic volatility and compared the best control variate between option, two contingent claims and stock using both Milstein method and mixing method to compare their performance. Lastly, we compared the simulation method using all control variates to the mixing method.

The rest of the report will be organized as follows. Chapter 2 will define the theoretical framework that is needed for this project. Chapter 3 will provide the mathematical derivations for simulations. Chapter 4 will describe the implementation of the numerical simulations, discuss the results, analysis and findings. Lastly, chapter 5 will summarize and give the conclusion of this report.

# 2 Theoretical Framework

## 2.1 Fundamental Setting

We are given that an asset price following the process $S = (S_t)_{t\geq 0}$ and its instantaneous variance $v = (v_t)_{t\geq 0}$ follow the Heston model, i.e., they satisfy the coupled SDE:

$$dS_t = S_t\sqrt{v_t}dW_t^S \quad \text{and} \quad dv_t = \kappa(\theta - v_t)dt + \eta\sqrt{v_t}dW_t^v$$

where $(W_t^S, W_t^v)_{t\geq 0}$ are correlated risk-neutral Brownian motions with correlation $\rho$.

Also, we are given the following base model parameters: $r = 0$, $S_0 = 1$, $\sqrt{v_0} = 20\%$, $\kappa = 3$, $\sqrt{\theta} = 40\%$, $\eta = 1.5$, and $\rho = -0.5$. We fix the number of simulations at 5,000, and the step size to be $\Delta t = \frac{1}{1000}$.

## 2.2 Implied Volatility

Note that under the Black-Scholes model, we have the underlying asset price $S_t$ satisfying the following SDE:

$$dS_t = S_t(\mu dt + \sigma dW_t)$$

where $\mu$ is the stock price drift, $\sigma$ is volatility as defined in fundamental settings and $W_t$ is a standard Brownian motion under the $\mathbb{P}$-measure.

At the same time, under Black-Scholes model assumptions, we calculate the European put and call option price at zero time as follows:

$$P^{BS}(S_T, K, r, \sigma, T) = \Phi(-d_-)Ke^{-rT} - \Phi(-d_+)S_T$$

$$C^{BS}(S_T, K, r, \sigma, T) = S_T\Phi(d_+) - Ke^{-rT}\Phi(d_-)$$

where $d_+ = \frac{log(\frac{S_T}{K})+(r+\frac{1}{2}\sigma^2)T}{\sigma\sqrt{T}}$, $d_- = \frac{log(\frac{S_T}{K})+(r-\frac{1}{2}\sigma^2)T}{\sigma\sqrt{T}} = d_+ - \sigma\sqrt{T}$, $S_T$ is the stock price at maturity $T$, other parameters as defined in fundamental settings.

Note that the implied volatility is not directly observable given the observed market option prices. With all other factors ($K$, $r$, $T$, $S_T$) known together with the observed market price, we can compute the implied volatility based on a put or call option by solving the following equations:

$$P_P^{MKT} = P^{BS}(S_T, K, r, \sigma, T)$$

or

$$P_C^{MKT} = C^{BS}(S_T, K, r, \sigma, T)$$

Where $P_P^{MKT}$ and $P_C^{MKT}$ are the observed market price of the corresponding put or call European option, $P^{BS}$ and $C^{BS}$ are the Black-Scholes model put or call European option price computed using implied volatility.

## 2.3 Numerical Solutions to Stochastic Differential Equations

A stochastic differential equation (SDE) can be written in a general form as,

$$dX_t = a(X_t, t)dt + b(X_t, t)dW_t \tag{1}$$

where $X_t$ is the stochastic process, $a(X_t, t)$ and $b(X_t, t)$ are coefficient functions for the differentials and $W_t$ is a standard Brownian motion. When determining the solution to an SDE, the analytical result may not exist or are able to be calculated easily, in such cases it can be beneficial to use an approximate numerical solution instead. There are a variety of numerical techniques that can be utilized to find numerical solutions to stochastic differential equations. The Euler discretization method and Milstein discretization method are of particular interest and will be discussed.

### 2.3.1 Euler Method

The Euler method constructs solutions to the SDE by discretizing the differentials and recursively uses the previous solution to build further solutions, beginning with the initial conditions.

The procedure is outlined as follows, assuming the initial condition, $X_0$, at time $t = 0$, to find the numerical solution to the SDE at a time $T$, time is first discretized into $N$ intervals where the discretized times $\tau$ obey the relation $0 = \tau_0 < \tau_1 < \ldots < \tau_N = T$. The differentials are then written as the difference between values in the next interval and the current interval. The numerical solution to the SDE, $Y$, is then,

$$Y_{n+1} = Y_n + a(Y_n, \tau_n)\Delta t + b(Y_n, \tau_n)\Delta W_n \tag{2}$$

where $n$ is the current interval and takes integer values $0 < n < N - 1$, the time intervals have width $\Delta t = \frac{T}{N}$ and the Brownian motion intervals $\Delta W_n = W_{\tau_{n+1}} - W_{\tau_n}$ follow a normal distribution with expected value zero and variance $\Delta t$. The Euler method solution at $T$ is $Y_N$ and is then used in place of the exact solution of $X_T$.

Similar to the Euler method for solving ordinary differential equations, the Euler method for solving SDE's is considered a rudimentary approach as it follows a basic discretization scheme, and its accuracy is highly dependent on the size of the discretized intervals. As such, for certain classes of SDE's, the more accurate Milstein SDE numerical solution method, is used.

### 2.3.2 Milstein Method

Consider a more restricted general form of a stochastic differential equation as,

$$dX_t = a(X_t)dt + b(X_t)dW_t \tag{3}$$

The key difference being that the coefficient functions are only functions of the stochastic

process, not of time itself.

The Milstein method finds numerical solutions to SDE's of this more restrictive general form. This is done similarly to the Euler method, but an extra correction term is included that is found using Ito's Lemma and taking the discretization to second order. The Milstein method can then be considered an extension of the Euler method for this more restrictive class of SDE's. The same discretization process and notion from the Euler method is used, and so will not be explained again. The resulting numerical solution to the SDE for the Milstein method is,

$$Y_{n+1} = Y_n + a(Y_n)\Delta t + b(Y_n)\Delta W_n + \frac{1}{2}b(Y_n)b'(Y_n)\left((\Delta W_n)^2 - \Delta t\right) \tag{4}$$

The extra term in the numerical solution allows for the variations due to the Brownian motion to be more accurately represented between time intervals. More concretely, the Milstein method has weak and strong convergence of order, $\Delta t$ whereas the Euler method has weak convergence of order, $\Delta t$ and strong convergence of order, $\sqrt{\Delta t}$. Therefore, the Milstein scheme has stronger convergence, leading to a more accurate numerical result for an equal number of intervals.

## 2.4 Heston Model

### 2.4.1 Model setup

The Heston model can be set up as a part of the stochastic volatility models, and it is generalized based on the Black-Scholes model, whereas the variance of asset returns is itself a variance process with stochastic nature. It's denoted as $v = (v_t)_{t\geq 0}$ and the volatility process is denoted as $\sqrt{v_t}$ respectively. The variance process is modelled using a Feller process, as the asset price and variance process satisfy the following $\mathbb{P}$-dynamics SDEs:

$$
\begin{aligned}
dS_t =& S_t\sqrt{v_t}dW_t \\
dv_t =& \kappa(\theta - v_t)dt + \eta\sqrt{v_t}dW_t^v
\end{aligned}
$$

Here, $W_t$ and $W_t^v$ are two correlated $\mathbb{P}$-Brownian motions with $d[W_t, W_t^v] = \rho dt$, so $\rho$ measures the correlation between two driving Brownian motions. Note that the parameter $\eta$ is a constant, representing the instantaneous volatility of the variance process, which is also known as vol-vol.

The variance process is defined to be positive if the Feller condition holds for $2\kappa\theta > \eta^2$, and according to the Feller process, the variance is mean reverting with mean-reversion level $\theta$ and rate $\kappa$ respectively.

### 2.4.2 Risk Neutral Dynamics

The $\mathbb{P}$-dynamics of the asset price and its variance are fully illustrated in the previous section, and we would like to further determine the $\mathbb{Q}$-dynamics of these processes to price claims, which requires the drifted versions of $W_t$ and $W_t^v$:

$$
\begin{aligned}
dW_t^{\mathbb{Q}} =& \lambda_t^S dt + dW_t \\
dW_t^{v\mathbb{Q}} =& \lambda_t^v dt + dW_t^v
\end{aligned}
$$

Therefore, the correct drift corrections that we must choose for $W_t$ and $W_t^v$ can be derived respectively. First, $\lambda^S$ must be chosen to ensure that the drift of the asset under the measure $\mathbb{Q}$ is equal to the risk-free rate $r$. Since the $\mathbb{Q}$-dynamics are given by:

$$
dS_t = - S_t\lambda_t^S\sqrt{v_t}dt + \sqrt{v_t}dW_t^{\mathbb{Q}}
$$

Through setting the drift term equal to $r$, we get the required drift correction, $\lambda_t^S = \frac{\mu - r}{\sqrt{v_t}}$. According to the fact that $v$ is not a traded asset, there are no additional no-arbitrage requirements that need to be satisfied, so $\lambda^v$ can be chosen freely. For a choice of $\lambda^v$, we can get the $\mathbb{Q}$-dynamics of the variance process to be:

$$dv_t = (\kappa(\theta - v_t) - \lambda_t^v \eta\sqrt{v_t})dt + \eta\sqrt{v_t}dW_t^{v\mathbb{Q}}$$

One approach is to choose $\lambda^v$ so that the functional form of the process is maintained. For example, by using $\lambda_t^v = a\sqrt{v_t} + \frac{b}{\sqrt{v_t}}$, the $\mathbb{Q}$-dynamics of the variance process can still be maintained to follow a Feller process:

$$\begin{aligned} dv_t &= \kappa^{\mathbb{Q}}(\theta^{\mathbb{Q}} - v_t)dt + \eta\sqrt{v_t}dW_t^{v\mathbb{Q}} \\ \kappa^{\mathbb{Q}} &= \kappa + a\eta \\ \theta^{\mathbb{Q}} &= \frac{\kappa\theta - b\eta}{\kappa + a\eta} \end{aligned}$$

In this case, the parameters $\mu$, $\kappa$, $\theta$ and $\eta$ describe the real-world dynamics of the asset price and variance processes, and the parameters $a$ and $b$ are degrees of freedom that allow us to calibrate the model to observed market prices, which minimize the difference between market prices and model-implied prices.

After determining the parameters, $\kappa^{\mathbb{Q}}$ and $\theta^{\mathbb{Q}}$ can be computed and they represent the market-implied mean reversion level and rate respectively. Therefore, the alternative drift adjustments leads to valid no-arbitrage prices based on the choice of $\lambda^v$.

## 2.5 Control Variate

A control variate is a technique used to reduce the variance of a Monte Carlo simulation when we have an analytic solution of a closely related model. Suppose that $X$ and $Y_1, \ldots, Y_m$ are random variables. Let $(X^{(n)}, Y_1^{(n)}, \ldots, Y_m^{(n)})_{n=1,\ldots,N}$ denote Monte Carlo simulations of $X$ and $Y_1, \ldots, Y_m$.

Given the analytical expression for $h_i = \mathbb{E}[Y_i]$ for $i = 1, \ldots, m$, the estimator of $g = \mathbb{E}[X]$,

denoted as $\hat{g}$ can be written as:

$$\hat{g} = \frac{1}{N}\sum_{n=1}^{N} X^{(n)} + \sum_{i=1}^{m} \gamma_i (h_i - \frac{1}{N}\sum_{n=1}^{N} Y_i^{(n)})$$

where $(\gamma_i)_{i=1,\dots,N}$ are arbitrary constants. Note that $\gamma_i = 0$ for $i = 1, \dots, m$ corresponds to usual Monte Carlo estimate setting.

Now suppose there are correlations between $X$ and $Y_i$. And we define a new random variable $H = X + \sum_{i=1}^{m} \gamma_i (h_i - Y_i)$. Then, the optimal $\gamma_i$ minimizes the variance of the newly introduced random variable $H$. Note that $\mathbb{E}[H] = \mathbb{E}[X]$ by construction, and therefore the equation for $\hat{g}$ defined above can be seen as the Monte Carlo estimate of $\mathbb{E}[H]$, thus, it can also be seen as the Monte Carlo estimate of $\mathbb{E}[X]$. The variance of this estimator is proportional to the variance of $H$ and therefore minimizing the variance of $H$. In this case, it minimizes the variance of the MC estimator of $\mathbb{E}[H]$, and therefore it also minimizes the variance of $\mathbb{E}[X]$.

The control variate technique described above can be applied to the Heston Model to generate the control variate option price to estimate implied volatility. Details will be discussed in later sections.

# 3 Mathematical Derivations

## 3.1 Heston Model

### 3.1.1 Euler Method

In section 3.1.1, 3.1.2 and 3.1.4 , we would like to implement three discretization techniques, including Euler discretization, Milstein discretization and the mixing method using Milstein discretization, which all aim to discretize the continuous-time stochastic process in the Heston model into a discrete time process. We would like to start off by showing the mathematical derivations involved in Euler discretization, which is the most straight-forward way

to discretize the process.

As mentioned earlier, the stochastic differential equation for stock price is $dS_t = S_t\sqrt{v_t}dW_t$. Under the assumption that the model is geometric-like, $x_t$ is defined as the log of stock price, whereas $d[S,S]_t$ represents the quadratic variation of $S$ and $t \in [t_{k-1}, t_k]$:

$$\begin{aligned} x_t =& log(S_t) = g(S_t) \\ dx_t =& g'(S_t)dS_t + \frac{1}{2}g''(S_t)d[S,S]_t \\ =& \frac{dS_t}{S_t} + \frac{1}{2}(-\frac{1}{S_t^2})S_t^2 v_t dt \\ =& -\frac{1}{2}v_t dt + \sqrt{v_t}dW_t \end{aligned}$$

Using the Euler discretization, we have the following relationship, whereas $Z_k^S$ is i.i.d., which follows $N \sim (0,1)$ distribution under the measure $\mathbb{Q}$:

$$\begin{aligned} x_{t_k} - x_{t_{k-1}} &= -\frac{1}{2}v_{t_{k-1}}\Delta t + \sqrt{v_{t_{k-1}}}(W_{t_k} - W_{t_{k-1}}) \\ x_{t_k} - x_{t_{k-1}} &\overset{\mathrm{d}}{=} -\frac{1}{2}v_{t_{k-1}}\Delta t + \sqrt{v_{t_{k-1}}\Delta t}Z_k^S \end{aligned}$$

Similarly, the continuous stochastic differential equation for variance process can be described as below. We can also apply the Euler discretization, whereas $Z_k^v$ is also i.i.d., which follows $N \sim (0,1)$ distribution:

$$\begin{aligned} dv_t &= \kappa(\theta - v_{t_{k-1}})dt + \eta_{t_{k-1}}\sqrt{v_{t_{k-1}}}dW_t^v \\ v_{t_k} - v_{t_{k-1}} &= \kappa(\theta - v_{t_{k-1}})\Delta t + \eta_{t_{k-1}}\sqrt{v_{t_{k-1}}}(dW_{t_k}^v - dW_{t_{k-1}}^v) \\ v_{t_k} - v_{t_{k-1}} &\overset{\mathrm{d}}{=} \kappa(\theta - v_{t_{k-1}})\Delta t + \eta_{t_{k-1}}\sqrt{v_{t_{k-1}}\Delta t}Z_k^v \end{aligned}$$

Therefore, we can further summarize the above results using the matrix form:

$$\begin{bmatrix} x_{t_k} - x_{t_{k-1}} \\ v_{t_k} - v_{t_{k-1}} \end{bmatrix} \overset{\mathrm{d}}{=} \begin{bmatrix} -\frac{1}{2}v_{t_{k-1}} \\ \kappa(\theta - v_{t_{k-1}}) \end{bmatrix} \Delta t + \begin{bmatrix} \sqrt{v_{t_{k-1}}\Delta t}Z_k^S \\ \eta_{t_{k-1}}\sqrt{v_{t_{k-1}}\Delta t}Z_k^v \end{bmatrix}$$

whereas

$$\begin{bmatrix} Z_k^S \\ Z_k^v \end{bmatrix} \sim N(\begin{bmatrix} 0 \\ 0 \end{bmatrix}, \begin{bmatrix} 1 & \rho \\ \rho & 1 \end{bmatrix})$$

### 3.1.2 Milstein Method

Comparing to Euler's method which requires a large computational time, the Milstein method can be applied toward the stochastic differential equation with the drift and volatility directly depending on stock price rather than time step. In this case, we have the following expressions with $a_t = f_a(y_t)$, $b_t = f_b(y_t)$ and $y_t = log(S_t)$ to distinguish from Euler method:

$$\begin{aligned} dy_t =& a_t dt + b_t dW_t \\ y_{t_k} - y_{t_{k-1}} =& \int_{t_{k-1}}^{t_k} a_u du + \int_{t_{k-1}}^{t_k} b_u dW_u \end{aligned}$$

Through expanding $b$ using Ito's Lemma, the Milstein method makes each increment unit more accurate and we can derive the following results by taking integration:

$$\begin{aligned} db_t =& (a_t \partial_y b(y_t) + \frac{1}{2} b_t^2 \partial_{yy} b(y_t))dt + b_t \partial_y b(y_t) dW_t \\ b_u =& b_{t_{k-1}} + \int_{t_{k-1}}^{u} (a_s \partial_y b(y_s) + \frac{1}{2} b_s^2 \partial_{yy} b(y_s))ds + \int_{t_{k-1}}^{u} b_s \partial_y b(y_s) dW_s \end{aligned}$$

Therefore, we can transform $y_{t_k} - y_{t_{k-1}}$ using the results above:

$$\begin{aligned} y_{t_k} - y_{t_{k-1}} \simeq& a_{t_{k-1}} \int_{t_{k-1}}^{t_k} du + \int_{t_{k-1}}^{t_k} (b_{t_{k-1}} + \int_{t_{k-1}}^{u} b_s \partial_y b(y_s) dW_s) dW_u \\ =& a_{t_{k-1}}(t_k - t_{k-1}) + b_{t_{k-1}}(W_{t_k} - W_{t_{k-1}}) + \int_{t_{k-1}}^{t_k} (\int_{t_{k-1}}^{u} b_s \partial_y b(y_s) dW_s) dW_u \end{aligned}$$

$$\begin{aligned} whereas \int_{t_{k-1}}^{t_k} b_u dW_u \simeq& \int_{t_{k-1}}^{t_k} (b_{t_{k-1}} + \int_{t_{k-1}}^{u} b_s \partial_y b(y_s) dW_s) dW_u \\ =& b_{t_{k-1}}(W_{t_k} - W_{t_{k-1}}) + b_{t_{k-1}} \partial_y b(y_{t_{k-1}}) \int_{t_{k-1}}^{t_k} (\int_{t_{k-1}}^{u} dW_s) dW_u \end{aligned}$$

Note that we have the following relationship to simplify the calculations through applying

Ito's Lemma:

$$\begin{aligned}
\int_{t_{k-1}}^{t_k}(\int_{t_{k-1}}^{u} dW_s)dW_u &= \int_{t_{k-1}}^{t_k}(W_u - W_{t_{k-1}})dW_u \\
&= \int_{t_{k-1}}^{t_k} W_u dW_u - W_{t_{k-1}}\int_{t_{k-1}}^{t_k} dW_u \\
&= \frac{1}{2}(W_u^2 - u)]_{t_{k-1}}^{t_k} - W_{t_{k-1}}(W_{t_k} - W_{t_{k-1}}) \\
&= \frac{1}{2}(W_{t_k}^2 - W_{t_{k-1}}^2 - (t_k - t_{k-1})) - W_{t_{k-1}}(W_{t_k} - W_{t_{k-1}}) \\
&= \frac{1}{2}(W_{t_k}^2 - 2W_{t_k}W_{t_{k-1}} + W_{t_{k-1}}^2 - (t_k - t_{k-1})) \\
&= \frac{1}{2}(\Delta W_t^2 - \Delta t)
\end{aligned}$$

Through bringing the results back to the original equation, $y_{t_k} - y_{t_{k-1}}$, we have:

$$y_{t_k} - y_{t_{k-1}} = a_{t_{k-1}}\Delta t + b_{t_{k-1}}\Delta W_t^2 + b_{t_{k-1}}\partial_y b(y_{t_{k-1}}) \times \frac{1}{2}(\Delta W_t^2 - \Delta t)$$

According to the Heston model, we have:

$$\begin{aligned}
dS_t &= S_t\sqrt{v_t}dW_t \\
dv_t &= \kappa(\theta - v_t)dt + \eta\sqrt{v_t}dW_t^v \\
y_t &= log(S_t) \\
dy_t &= -\frac{1}{2}v_t dt + \sqrt{v_t}dW_t
\end{aligned}$$

As a result, the Milstein discretization can be derived as the following and the asset price dynamics remains the same as Euler method:

$$\begin{aligned}
y_{t_k} - y_{t_{k-1}} &\overset{\mathrm{d}}{=} -\frac{1}{2}v_{t_{k-1}}\Delta t + \sqrt{v_{t_{k-1}}\Delta t}Z_k^S \\
v_{t_k} - v_{t_{k-1}} &\overset{\mathrm{d}}{=} \kappa(\theta - v_{t_{k-1}})\Delta t + \eta\sqrt{v_{t_{k-1}}\Delta t}Z_k^v + \frac{1}{4}\eta^2\Delta t(Z_k^{v^2} - 1) \\
\begin{bmatrix} y_{t_k} - y_{t_{k-1}} \\ v_{t_k} - v_{t_{k-1}} \end{bmatrix} &\overset{\mathrm{d}}{=} \begin{bmatrix} -\frac{1}{2}v_{t_{k-1}} \\ \kappa(\theta - v_{t_{k-1}}) \end{bmatrix}\Delta t + \begin{bmatrix} \sqrt{v_{t_{k-1}}\Delta t}Z_k^S \\ \eta\sqrt{v_{t_{k-1}}\Delta t}Z_k^v \end{bmatrix} + \begin{bmatrix} 0 \\ \frac{1}{4}\eta^2\Delta t(Z_k^{v^2} - 1) \end{bmatrix}
\end{aligned}$$

### 3.1.3 Mixing Method

In this subsection, we would like to implement the mixing method using Milstein discretization of $v_{t_k}$. From previous results, the Milstein method gives:

$$v_{t_k} \overset{\mathrm{d}}{=} v_{t_{k-1}} + \kappa(\theta - v_{t_{k-1}})\Delta t + \eta\sqrt{v_{t_{k-1}}\Delta t}Z_k^v + \frac{1}{4}\eta^2\Delta t(Z_k^{v^2} - 1)$$

Conditional on the variance path derived through Milstein Method, the mixing method asset price process can be shown as the following:

$$\begin{aligned} W_t =& \rho W_t^v + \sqrt{1-\rho^2}W_t^{v\perp} \\ x_T - x_t =& -\frac{1}{2}\int_t^T v_u du + \int_t^T \sqrt{v_u}\rho dW_u^v + \int_t^T \sqrt{v_u(1-\rho^2)}dW_u^{v\perp} \end{aligned}$$

Given the fact that $Var(\int_t^T \sqrt{v_u(1-\rho^2)}dW_u^{v\perp}) = (1-\rho^2)\int_t^T v_u du$, the price process can be rewritten as the following, whereas $Z^\perp$ follows $N \sim (0,1)$ distribution:

$$x_T = x_t - \frac{1}{2}\int_t^T v_u du + \int_t^T \sqrt{v_u}\rho dW_u^v + \sqrt{(1-\rho^2)\int_t^T v_u du}Z^\perp$$

### 3.1.4 An Example of Derivative Valuation

To price derivatives under the Heston model, we can proceed in the usual manner, via an expectation or a PDE-based approach. As a continuation of previous part, 3.1.3, we would like to expand the analysis regarding European options. Here, we also use $x_t$ to represent the price of the underlying asset at time t.

$$\begin{aligned} x_t =& log(S_t) \\ dx_t =& -\frac{1}{2}v_t dt + \sqrt{v_t}dW_t \end{aligned}$$

Since $S$ doesn't explicitly show up in this SDE, we can use simulation of $x_t$ and $v_t$ to obtain the set of evolution paths in later sections and compute the expected value of call or put price respectively under the $\mathbb{Q}$-martingale measure. Here, we are taking the expectation of

call as an example:

$$C = \mathbb{E}^{\mathbb{Q}}[(S_T - K)_+] = \mathbb{E}^{\mathbb{Q}}[\mathbb{E}^{\mathbb{Q}}[(S_T - K)_+ | \sigma((v_u)_{u\in[0,T]})]]$$

Note that the notation $\sigma$ represents the $\sigma$-algebra. To compute the inner expectation, if $B_t$ and $W_t$ are independent ($\perp$) with each other, conditional on each path of $v$ leads to:

$$x_T|_\sigma \overset{\mathrm{d}}{=} X_0 e^{-\frac{1}{2}\int_0^T v_u du + (\int_0^T v_u du)^{\frac{1}{2}} Z}$$

Here, $Z$ follows $N \sim (0, 1)$ distribution under the measure $\mathbb{Q}$.

If $B_t$ and $W_t$ are two correlated Brownian motions, $Z_t$ can be defined as $\frac{W_t - \rho B_t}{\sqrt{1-\rho^2}}$, which refers to the Cholesky decomposition. Note that $Z_t$ is also a Brownian motion and $B_t$ and $Z_t$ are independent ($\perp$) with each other. Therefore, the expression of $dx_t$ can be further rewritten as:

$$\begin{aligned} W_t =& \rho B_t + \sqrt{1-\rho^2} Z_t \\ dx_t =& -\frac{1}{2} v_t dt + \sqrt{v_t}(\rho dB_t + \sqrt{1-\rho^2} dZ_t) \\ =& (-\frac{1}{2} v_t dt + \sqrt{v_t}\sqrt{1-\rho^2} dZ_t) + \sqrt{v_t}\rho dB_t \end{aligned}$$

As a result, we can obtain the following result by integrating through 0 to $T$:

$$x_T - x_0 = (-\frac{1}{2}\int_0^T v_u du + \sqrt{1-\rho^2}\int_0^T \sqrt{v_u} dZ_u) + \int_0^T \sqrt{v_u}\rho dB_u$$

Note that the sigma algebra associated with different paths are the same between $v_u$ and $B_u$: $\sigma((v_u)_{u\in[0,T]}) = \sigma((B_u)_{u\in[0,T]})$. Conditioning on the defined $\sigma$-algebra, we have the following distribution:

$$x_T - x_0|_\sigma \sim N(-\frac{1}{2}\int_0^T v_u du + \rho\int_0^T \sqrt{v_u} dB_u, (1-\rho^2)\int_0^T v_u du) = N(a, b^2)$$

Therefore, we can express $S_T$ as the following, where $N$ follows $N \sim (0, 1)$ distribution under

the measure $\mathbb{Q}$:

$$S_T|_\sigma \overset{\mathrm{d}}{=} F_0 e^{a+bN} = (S_0 e^{a+\frac{1}{2}b}) e^{-\frac{1}{2}b+bN}$$

This makes the expression equivalent of a Black-Scholes with zero interest rate and $\sigma^2 T = b^2$. Note that $\tilde{S_0} = S_0 e^{a+\frac{1}{2}b}$ is used to represent the new effective price.

As a result, the previous expectation can be written in a Black-Scholes form:

$$\begin{aligned} C =& \mathbb{E}^{\mathbb{Q}}[(S_T - K)_+ | \sigma] = \tilde{S_0}\Phi(d_+) - \kappa\Phi(d_-) \\ d_\pm =& \frac{log(\frac{\tilde{S_0}}{\kappa}) \pm b^2}{b} \end{aligned}$$

In conclusion, the Euler and Milstein method have been described previously and the mixing method is simply the Black-Scholes form of the option valuation in the Heston model as seen above. The naming convention comes from the fact that the Heston model is partially solved analytically, and the remaining unknown stochastic process, the stochastic volatility, is simulated using numerical methods. The mixing method is set through conditioning on a path of $v$, getting a Black-Scholes-like asset price and then averaging over those prices by different simulations. To simulate paths of $v$, we aim to approximate the integrals for a given path that gives a particular value of $a$ and $b$ at that path. Then, we consider to take expectation, which is more efficient than jointly simulating $x_t$ and $B_t$, and estimating the average of $S_T - K$ over all those simulations.

To compare their effects using Monte Carlo simulation, we utilize the following base parameters: $r = 0$, $S_0 = 1$, $v_0 = 20\%$, $\kappa = 3$, $\sqrt{\theta} = 40\%$, $\eta = 1.5$, $\rho = -0.5$. Throughout the process of generating the variance process over time, we fix the number of simulations at 5,000 and the step size to be $\Delta t = \frac{1}{1000}$.

## 3.2 Control Variate and the Optimal Choice of $\gamma_i$

As we discussed in section 2.5, when using the control variate technique to reduce the variance of a Monte Carlo simulation, we have to first determine the (model independent) expression of the optimal choice of $\gamma_i$ to minimize the variance of control variate estimate for the option price. Note that the variance of the random variable $H = X + \sum_{i=1}^{m} \gamma_i(h_i - Y_i)$, where $X$ and $Y_1, \cdots, Y_m$ are random variables (not necessarily independent) and $h_i = \mathbb{E}[Y_i]$ for $i = 1, \cdots, m$, can be calculated as follows:

$$
\begin{aligned}
Var(H) &= Var(X + \sum_{i=1}^{m} \gamma_i(h_i - Y_i)) \\
&= Var(X) + Var(\sum_{i=1}^{m} \gamma_i(h_i - Y_i)) + 2Cov(X, \sum_{i=1}^{m} \gamma_i(h_i - Y_i)) \\
&= Var(X) + \mathbb{E}[(\mathbb{E}[\sum_{i=1}^{m} \gamma_i(h_i - Y_i)] - \sum_{i=1}^{m} \gamma_i(h_i - Y_i))^2] \\
&+ 2\mathbb{E}[(X - \mathbb{E}[X])(\sum_{i=1}^{m} \gamma_i(h_i - Y_i) - \mathbb{E}[\sum_{i=1}^{m} \gamma_i(h_i - Y_i)])] \\
&\text{(Plugging in } h_i = \mathbb{E}[Y_i]) \\
&= Var(X) + \mathbb{E}[(\mathbb{E}[\sum_{i=1}^{m} \gamma_i \mathbb{E}[Y_i]] - \mathbb{E}[\sum_{i=1}^{m} \gamma_i Y_i] - \sum_{i=1}^{m} \gamma_i \mathbb{E}[Y_i] + \sum_{i=1}^{m} \gamma_i Y_i)^2] \\
&+ 2\mathbb{E}[(X - \mathbb{E}[X])(\sum_{i=1}^{m} \gamma_i \mathbb{E}[Y_i] - \sum_{i=1}^{m} \gamma_i Y_i - \mathbb{E}[\sum_{i=1}^{m} \gamma_i \mathbb{E}[Y_i]] + \mathbb{E}[\sum_{i=1}^{m} \gamma_i Y_i])]
\end{aligned}
$$

(Note that $\mathbb{E}[\mathbb{E}[Y_i]] = \mathbb{E}[Y_i]$, and $\gamma_i's$ are constants)

$$
\begin{aligned}
&= Var(X) + \mathbb{E}[(\sum_{i=1}^{m} \gamma_i \mathbb{E}[Y_i] - \mathbb{E}[\sum_{i=1}^{m} \gamma_i Y_i] - \sum_{i=1}^{m} \gamma_i \mathbb{E}[Y_i] + \sum_{i=1}^{m} \gamma_i Y_i)^2] \\
&+ 2\mathbb{E}[(X - \mathbb{E}[X])(\sum_{i=1}^{m} \gamma_i \mathbb{E}[Y_i] - \sum_{i=1}^{m} \gamma_i Y_i - \sum_{i=1}^{m} \gamma_i \mathbb{E}[Y_i] + \sum_{i=1}^{m} \gamma_i \mathbb{E}[Y_i])] \\
&= Var(X) + \mathbb{E}[(\sum_{i=1}^{m} \gamma_i Y_i - \mathbb{E}[\sum_{i=1}^{m} \gamma_i Y_i])^2] - 2\mathbb{E}[(X - \mathbb{E}[X])(\sum_{i=1}^{m} \gamma_i Y_i - \sum_{i=1}^{m} \gamma_i \mathbb{E}[Y_i])] \\
&= Var(X) + Var(\sum_{i=1}^{m} \gamma_i Y_i) - Cov(X, \sum_{i=1}^{m} \gamma_i Y_i) \\
&= Var(X) + \sum_{i=1}^{m} \gamma_i^2 Var(Y_i) + 2\sum_{i<j} \gamma_i \gamma_j Cov(Y_i, Y_j) - 2\sum_{i=1}^{m} \gamma_i Cov(X, Y_i)
\end{aligned}
$$

Taking partial derivative of $Var(H)$ w.r.t. $\gamma_i$ gives us:

$$\frac{\partial Var(H)}{\partial \gamma_i} = 2\gamma_i Var(Y_i) - 2Cov(X, Y_i) + 2\sum_{j=1, j\neq i}^{m} \gamma_j Cov(Y_i, Y_j)$$

Setting the above partial derivative to 0 gives us the candidate for $\gamma_i$ as follows:

$$
\begin{aligned}
&\frac{\partial Var(H)}{\partial \gamma_i} = 0 \\
&\Rightarrow 2\gamma_i Var(Y_i) - 2Cov(X, Y_i) + 2\sum_{j=1, j\neq i}^{m} \gamma_j Cov(Y_i, Y_j) = 0 \quad (\star) \\
&\Rightarrow \gamma_i = \frac{Cov(X, Y_i) - \sum_{j=1, j\neq i}^{m} \gamma_i Cov(Y_i, Y_j)}{Var(Y_i)}
\end{aligned}
$$

Note that $Var(Y_i) \neq 0$ otherwise $Y_i$ would be a constant.

Moreover, we calculate the second order partial derivative of $Var(H)$ w.r.t. $\gamma_i$ as:

$$\frac{\partial^2 Var(H)}{\partial \gamma_i^2} = 2Var(Y_i) \geq 0$$

Therefore, we verify that the calculated $\gamma_i$ minimizes $Var(H)$ as we desired. Thus, we got the (model independent) expression for the optimal choice of $\gamma_i$ as

$$\gamma_i = \frac{Cov(X, Y_i) - \sum_{j=1, j\neq i}^{m} \gamma_i Cov(Y_i, Y_j)}{Var(Y_i)}$$

Additionally, if we rearrange equation $(\star)$, we get:

$$\sum_{j=1}^{m} \gamma_i Cov(Y_i, Y_j) = Cov(X, Y_i)$$

$$\Rightarrow \Big[Cov(Y_i, Y_1) \cdots Cov(Y_i, Y_m)\Big] \begin{bmatrix} \gamma_1 \\ \vdots \\ \gamma_m \end{bmatrix} = Cov(X, Y_i)$$

Therefore, suppose we have $k$ control variate, then we know the vector of the optimal choice of $\gamma_i$ for $i = 1, \cdots, k$ satisfies the following equation:

$$\begin{bmatrix} Cov(Y_1, Y_1) & \cdots & Cov(Y_1, Y_k) \\ \vdots & \ddots & \vdots \\ Cov(Y_k, Y_1) & \cdots & Cov(Y_k, Y_k) \end{bmatrix} \begin{bmatrix} \gamma_1 \\ \vdots \\ \gamma_k \end{bmatrix} = \begin{bmatrix} Cov(X, Y_1) \\ \vdots \\ Cov(X, Y_k) \end{bmatrix}$$

where $\begin{bmatrix} \gamma_1 \\ \vdots \\ \gamma_k \end{bmatrix}$ is the vector of optimal choice of $\gamma_i$ for $i = 1, \cdots, k$.

## 3.3 Analytical Closed-form Expressions for Heston Model

When $v_t$ is replaced by $\bar{v}_t := \mathbb{E}[v_s]$ in the Heston model, we would like to derive the price of an option in the resulting deterministic volatility model in this section.

Similar to the standard Heston model, the asset price and variance process satisfy the fol-

lowing SDEs:

$$\begin{aligned} dS_t =& S_t\sqrt{\bar{v}_t}dW_t \\ d\bar{v}_t =& \kappa(\theta - \bar{v}_t)dt \end{aligned}$$

In order to obtain the expression further, we need to apply Ito's Lemma by taking $x_t = log(S_t)$. Consequently, we can obtain the following results:

$$\begin{aligned} x_t &= log(S_t) \\ &\rightarrow \frac{dx_t}{dS_t} = \frac{1}{S_t} \\ &\rightarrow \frac{d^2x_t}{dS_t^2} = -\frac{1}{S_t^2} \\ dx_t &= -\frac{1}{2} \times \frac{1}{S_t^2} \times S_t^2\bar{v}_t dt + S_t\sqrt{\bar{v}_t}\frac{1}{S_t}dW_t \\ &= -\frac{1}{2}\bar{v}_t dt + \sqrt{\bar{v}_t}dW_t \end{aligned}$$

By taking integration, we have:

$$\begin{aligned} x_t &= x_0 - \int_0^t \frac{1}{2}\bar{v}_s ds + \int_0^t \sqrt{\bar{v}_s}dW_s \\ S_t &= S_0 e^{-\int_0^t \frac{1}{2}\bar{v}_s ds + \int_0^t \sqrt{\bar{v}_s}dW_s} \end{aligned}$$

Using the relationship $\bar{v}_s = v_0 e^{-\kappa s} + \theta(1 - e^{-\kappa s}) = (v_0 - \theta)e^{-\kappa s} + \theta$, we can rewrite $S_t$ as:

$$\begin{aligned} S_t &= S_0 e^{-\int_0^t \frac{1}{2}((v_0-\theta)e^{-\kappa s}+\theta)ds + \int_0^t \sqrt{\bar{v}_s}dW_s} \\ &= S_0 e^{\int_0^t \frac{1}{2}((v_0-\theta)e^{-\kappa s}+\theta)d(-s) + \int_0^t \sqrt{\bar{v}_s}dW_s} \\ &= S_0 e^{\frac{1}{2}(v_0-\theta)\int_0^t e^{-\kappa s}d(-s) + \frac{1}{2}\theta\int_0^t 1d(-s) + \int_0^t \sqrt{\bar{v}_s}dW_s} \\ &= S_0 e^{\frac{1}{2\kappa}(v_0-\theta)(e^{\kappa t}-1) - \frac{1}{2}\theta t + \int_0^t \sqrt{\bar{v}_s}dW_s} \end{aligned}$$

Setting $t = T$ gives us:

$$S_T = S_0 e^{\frac{1}{2\kappa}(v_0-\theta)(e^{\kappa T}-1) - \frac{1}{2}\theta T + \int_0^T \sqrt{\bar{v}_s}dW_s}$$

Note that we have:

$$\begin{aligned}
\mathbb{E}[\int_0^T \sqrt{\bar{v}_s} dW_s] &= 0 \\
Var(\int_0^T \sqrt{\bar{v}_s} dW_s) &= \mathbb{E}[(\int_0^T \sqrt{\bar{v}_s} dW_s - \mathbb{E}[\int_0^T \sqrt{\bar{v}_s} dW_s])^2] \\
&= \mathbb{E}[(\int_0^T \sqrt{\bar{v}_s} dW_s)^2] \\
&= \int_0^T (\sqrt{\bar{v}_2})^2 ds \quad \text{(by Ito's Isometry)} \\
&= \int_0^T (v_0 - \theta) e^{-\kappa s} + \theta ds \\
&= \int_0^T -(v_0 - \theta) e^{-\kappa s} d(-s) + \int_0^T \theta ds \\
&= -\frac{1}{k}(v_0 - \theta)(e^{\kappa T} - 1) + \theta(T - 0) \\
&= \frac{1}{k}(\theta - v_0)(e^{\kappa T} - 1) + \theta T
\end{aligned}$$

Therefore, $\int_0^T \sqrt{\bar{v}_s} dW_s$ can be written as $\sigma_{\bar{v}_s} Z$, where $\sigma^2_{\bar{v}_s} = \frac{1}{\kappa}(\theta - v_0)(e^{\kappa T} - 1) + \theta T$, and $Z \sim N(0, 1)$. Thus, we have:

$$\begin{aligned}
S_T &= S_0 e^{\frac{1}{2\kappa}(v_0 - \theta)(e^{\kappa T} - 1) - \frac{1}{2}\theta T + \sigma_{\bar{v}_s} Z} \\
&= S_0 e^{-\frac{1}{2}(\frac{1}{\kappa}(\theta - v_0)(e^{\kappa T} - 1) + \theta T) + \sigma_{\bar{v}_s} Z} \\
&= S_0 e^{-\frac{1}{2}\sigma^2_{\bar{v}_s} + \sigma_{\bar{v}_s} Z}
\end{aligned}$$

where $\sigma^2_{\bar{v}_s} = \frac{1}{\kappa}(\theta - v_0)(e^{\kappa T} - 1) + \theta T$.

Since we aim to price an option in the resulting volatility model derived in closed form, we can bring the expression of $S_T$ toward the Black-Scholes call and put option price obtained in Section 2.2. Note that since $r = 0$, $e^{-rT} = 1$.

$$\begin{aligned}
P^{BS} &= K\Phi(-d_-) - S_0\Phi(-d_+) \\
C^{BS} &= S_0\Phi(d_+) - K\Phi(d_-)
\end{aligned}$$

where $d_+ = \frac{log(\frac{S_0}{K})+\sigma^2_{\bar{v}_s}}{\sigma_{\bar{v}_s}}$, $d_- = \frac{log(\frac{S_0}{K})-\sigma^2_{\bar{v}_s}}{\sigma_{\bar{v}_s}}$, and $\sigma^2_{\bar{v}_s} = \frac{1}{k}(\theta - v_0)(e^{kT} - 1) + \theta T$.

## 3.4 Value of a Contingent Claim

### 3.4.1 Paying $\int_0^T v_s ds$ at maturity $T$

In this section, we would like to derive the value of a contingent claim paying $\int_0^T v_s ds$ at maturity $T$ and further validate the analytic calculation using Milstein simulations in later section.

$$
\begin{aligned}
V &= \mathbb{E}[\int_0^T v_s ds] \\
&= \mathbb{E}[\int_0^T v_s ds] \\
&= \int_0^T \mathbb{E}[v_s] ds \\
&\text{Given the fact that } \bar{v}_t := \mathbb{E}[v_t] \\
&= \int_0^T \bar{v}_s ds \\
&= \int_0^T v_0 e^{-\kappa s} + \theta(1 - e^{-\kappa s}) ds \\
&= (-(\frac{V_0 e^{-\kappa T}}{\kappa}) + \theta T + \frac{\theta}{\kappa} e^{-\kappa T} + \frac{V_0}{\kappa} - \frac{\theta}{\kappa}) \\
&= (\frac{V_0 - \theta}{\kappa}(1 - e^{-\kappa T}) + \theta T)
\end{aligned}
$$

So, $V = \frac{V_0 - \theta}{\kappa}(1 - e^{-\kappa T}) + \theta T$.

### 3.4.2 Paying $\int_0^T v_s^2 ds$ at maturity $T$

In this section, we would like to derive the value of a contingent claim paying $\int_0^T v_s^2 ds$ at maturity $T$ and further validate the analytic calculation using Milstein simulations in later section.

$$
\begin{aligned}
V &= \mathbb{E}[\int_0^T v_s^2 ds] \\
&= \mathbb{E}[\int_0^T v_s^2 ds] \\
&= \int_0^T \mathbb{E}[v_s^2] ds
\end{aligned}
$$

In order to obtain the expression of $\mathbb{E}[v_s^2]$, we need to apply Ito's Lemma by assuming $f(t, v_t) = v_t^2$.

Consequently, we have:

$$
\begin{aligned}
f(t, v_t) &= v_t^2 \\
\Rightarrow \frac{\partial f(t, v_t)}{\partial v_t} &= 2v_t \\
\Rightarrow \frac{\partial^2 f(t, v_t)}{\partial v_t^2} &= 2
\end{aligned}
$$

Note that $dv_t = \kappa(\theta - v_t)dt + \eta\sqrt{v_t}dW_t$. By Ito's Lemma, we have:

$$
\begin{aligned}
dv_t^2 &= \kappa(\theta - v_t) \times \frac{\partial f(t, v_t)}{\partial v_t} dt + \frac{1}{2} \times \frac{\partial^2 f(t, v_t)}{\partial v_t^2} \times (\eta\sqrt{v_t})^2) dt + \eta\sqrt{v_t} \times \frac{\partial f(t, v_t)}{\partial v_t} dW_t^v \\
&= (\kappa(\theta - v_t) \times 2v_t + \frac{1}{2} \times 2 \times (\eta\sqrt{v_t})^2) dt + \eta\sqrt{v_t} \times 2v_t dW_t^v \\
&= ((2\kappa\theta + \eta^2)v_t - 2\kappa v_t^2) dt + 2\eta v_t \sqrt{v_t} dW_t^v
\end{aligned}
$$

Therefore, we can integrate upon the formula above and take it's expectation to obtain $\mathbb{E}[v_s^2]$:

$$
\begin{aligned}
v_t^2 &= v_0^2 + \int_0^t ((2\kappa\theta + \eta^2)v_s - 2\kappa v_s^2) ds + 2\int_0^t \eta v_s \sqrt{v_s} dW_s^v \\
\mathbb{E}[v_s^2] &= \mathbb{E}[v_0^2] + \int_0^t ((2\kappa\theta + \eta^2)\bar{v}_s - 2\kappa\mathbb{E}(v_s^2)) ds
\end{aligned}
$$

Then we have:

$$
\begin{cases}
\dfrac{d\mathbb{E}(v_t^2)}{dt} = (2\kappa\theta + \eta^2)\bar{v}_s - 2\kappa\mathbb{E}(v_t^2) \\
\mathbb{E}(v_t^2)|_{t=0} = v_0^2
\end{cases}
$$

Solving the linear ODE with boundary condition using general solution, we have:

$$\mathbb{E}(v_t^2) = (v_0^2 - \frac{(2\kappa\theta+\eta^2)(v_0-\theta)}{\kappa} - \frac{(2\kappa\theta+\eta^2)\theta}{2\kappa})e^{-2\kappa t} + \frac{(2\kappa\theta+\eta^2)(v_0-\theta)}{\kappa}e^{-\kappa t} + \frac{(2\kappa\theta+\eta^2)\theta}{2\kappa}$$

Then we have the following value function under $r = 0$:

$$\begin{aligned} V &= \int_0^T \mathbb{E}[v_s^2]ds \\ &= \int_0^T (v_0^2 - \frac{(2\kappa\theta+\eta^2)(v_0-\theta)}{\kappa} - \frac{(2\kappa\theta+\eta^2)\theta}{2\kappa})e^{-2\kappa s} + \frac{(2\kappa\theta+\eta^2)(v_0-\theta)}{\kappa}e^{-\kappa s} + \frac{(2\kappa\theta+\eta^2)\theta}{2\kappa})ds \\ &= (v_0^2 - \frac{(2\kappa\theta+\eta^2)(v_0-\theta)}{\kappa} - \frac{(2\kappa\theta+\eta^2)\theta}{2\kappa})\frac{1-e^{-2\kappa T}}{2\kappa} + (2\kappa\theta+\eta^2)(v_0-\theta)\frac{1-e^{-\kappa T}}{\kappa^2} + \frac{(2\kappa\theta+\eta^2)\theta T}{2\kappa} \end{aligned}$$

# 4 Implementation, Results and Analysis

## 4.1 Implied Volatilities from Direct Numerical Solutions to the Heston Model

Understanding how to solve for implied volatilites and constructing an implied volatility surface for different option strike prices and maturities is fundamental in determining how the Black-Scholes Model differs from actual market option values and other model option values. Specifically, investigating the implied volatilities when comparing the Black-Scholes model with the Heston model allows for the construction of volatility surfaces and smiles in a straight-forward manner without the need for direct market data. Solving the Heston model also allows for investigating the different techniques that can be used to construct simulated numerical solutions to the model. The stochastic volatility process will be solved using the Milstein method for SDE's and the asset price process will be solved using the Euler method for SDE's and then using the mixing method for the Heston model. The implied volatility smiles and surface will be constructed from put options when the strike price, $K$, is less than the initial asset price, $S_0$, (i.e. $K < S_0$) and call options when the strike price is equal to or greater than the initial asset price (i.e. $K \geq S_0$). The different option types are used

to lower the possibility that the option value is zero for the majority of the option lifetime. The implied volatility is determined for options with strike prices $K = 0.8, 0.85, \ldots, 1.2$ and maturities, $T = \frac{1}{4}, \frac{1}{2}, 1$ which are used to construct the implied volatility smiles and surfaces.

Before the simulations can be performed to find the implied volatility, the explicit form of the numerical solution to the logarithm of the asset price, $x_t = \log(S_t)$ using the Euler method and the numerical solution to stochastic volatility, $v_t$, using the Milstein method must be found. From section 2.3 the general form of SDE solutions for the Euler and Milstein method can be found, to implement these solutions to the Heston model one only need to compare the coefficient functions. However, to account for correlations in the Brownian motions in the Heston model, the Brownian Motion for the asset price can be written as,

$$W_t^S = \rho W_t^v + \sqrt{1-\rho^2} Z_t \tag{5}$$

where $Z_t$ is an independent standard Brownian motion. Using the Euler method, the logarithm of the asset price is,

$$x_{t+\Delta t} = x_t - \frac{1}{2}(v_t)_+ \Delta t + \sqrt{(v_t)_+} \Delta W_t^s \tag{6}$$

and the stochastic volatility using the Milstein method is,

$$v_{t+\Delta t} = (v_t)_+ + \kappa \left(\theta - (v_t)_+\right) \Delta t + \eta \sqrt{(v_t)_+} \Delta W_t^v + \frac{1}{4}\eta^2 (\Delta W_t^v - \Delta t) \tag{7}$$

where $(v_t)_+ = max(v_t, 0)$ so that volatilities can not be negative and therefore the Heston model is still valid. With the Euler method form of the log asset price, the asset price itself can be found by exponentiating the results and the usual form for valuing a European style option under the risk-neutral measure, $\mathbb{Q}$, is used to find the Heston model option value. That is for a call option,

$$C = \mathbb{E}^{\mathbb{Q}} \left[ (S_T - K)_+ \right] \tag{8}$$

and for a put option,

$$P = \mathbb{E}^{\mathbb{Q}} \left[ (K - S_T)_+ \right]. \tag{9}$$

The form of the call and put option value in the Heston model using the mixing method has already been derived in section 3.1.4 and so will not be repeated. With the option values for the Heston model, the implied volatility is found by solving for the Black-Scholes volatility that makes its option value the same as the Heston model's option value. The simulation results for the implied volatility using the Euler method and the Milstein method, which will be called the discretization approach, will first be investigated.

### 4.1.1 Discretization Approach

To investigate the implied volatilities under the Heston model using the discretization approach to solve the stochastic processes, the implied volatility surface for different strikes and maturities will be examined, as will the volatility smiles, that is fixing the maturity how does the implied volatility change as a function of strike price. The plot of the volatility smile for an option with maturity $T = \frac{1}{4}$ is given below. In all volatility smile plots, the confidence interval is the $95^{th}$ percentile, that is between the upper and lower quantile, 95% of the simulation values lie in that region.

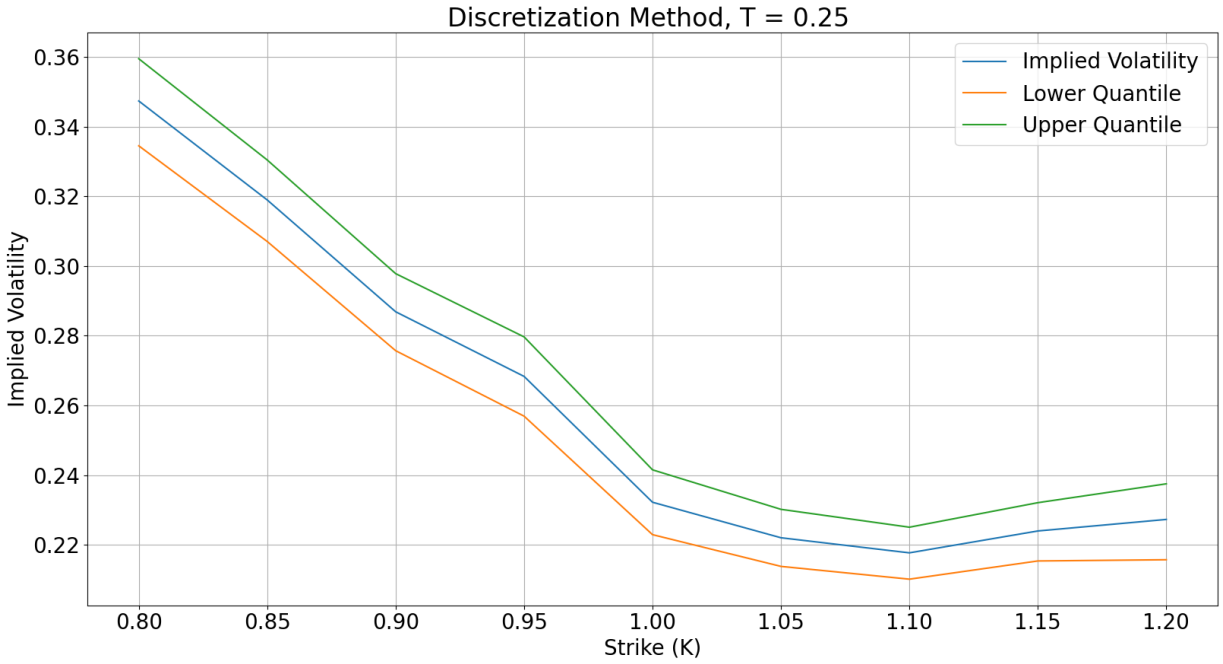


**Figure 1:** Changes to implied volatility as a function of the strike price for fixed maturity $T = \frac{1}{4}$. The volatility smile appears more so as a smirk, with the implied volatility being positively skewed for the domain of strikes where it has been calculated.

It can be seen from the above plot that the volatility smile does not have smooth transitions in the implied volatility between different strike prices. This volatility smile does not have the same parabolic-like smooth shape as seen in typical reference material on volatility smiles. The difference in the shapes can be explained due to the fact that the strike price step size was quite coarse and that the discretization method is an approximation that uses a finite number of simulations and time intervals, and so it may not be representing the true option price structure of the Heston model. To improve these results, a finer strike price step size may be implemented as well as a greater number of simulations and time intervals or an improved numerical approximation method. Observing the confidence interval, it can be seen that it remains consistent throughout the different strike prices and has a band size of about, 0.03 considering the range of the implied volatilites is in the neighbourhood of 0.3 this corresponds to about a 10% variation in order to capture 95% of the simulated values. This proves the earlier suspicion that the numerical accuracy of the discretization method is effecting the results for the volatility smile. The range and values of the implied volatilities

seem reasonable, none are negative or extremely close to zero and none are close to one. It can be argued that we suspect these results to be reasonable as the strike price is close to the initial asset price and that the parameters of the Heston model and the model itself is well studied and implemented to investigate markets. So, we would expect for this type of model it would not exhibit exotic behaviour in terms of implied volatilites which is the case and can be seen in the plot.

The plot of the volatility smile for fixed maturity $T = 1$ will now be investigated. However, it should be noted that the volatility smile for a maturity $T = \frac{1}{2}$ can be found in the appendix and is not included in the main sections of the report, as it does not add significant insights that have already been gained from the $T = \frac{1}{4}$ and $T = 1$ maturity volatility smiles. The $T = 1$ volatility smile is given below,

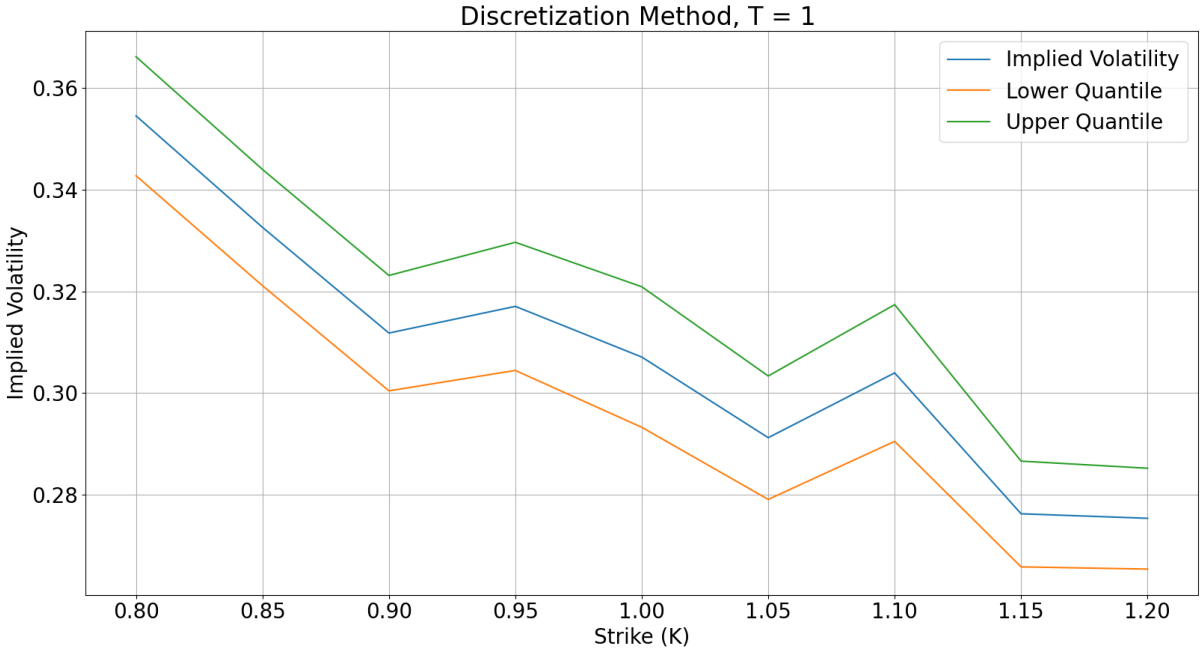


**Figure 2:** Changes to implied volatility as a function of the strike price for fixed maturity $T = 1$. The volatility smile appears more so as a decreasing trend rather than a smirk or smile, with the implied volatility being positively skewed for the domain of strikes where it has been calculated.

It can be seen from the plot that the transition between strike prices is even less smooth compared to the $T = \frac{1}{4}$ maturity plot and that the overall expected parabolic shape is even

less obvious. An explanation for this is that for options with greater maturities, the implied volatility is less dependent on the stock price, this is evident in the plot above as the range of implied volatilities is around 0.08 whereas the range is around 0.13 for the $T = \frac{1}{4}$ plot. So, for a decreased range of values, the variations between strike prices due to inaccuracies in the numerical method become more prominent, and they are seen in the $T = 1$ plot where the implied volatility increases for greater strike prices when the implied volatility trend indicates that it should actually be decreasing. It can also be seen that the confidence interval is similar in band size to the $T = \frac{1}{4}$ plot.

The complete implied volatility surface for different strike prices and maturities is now investigated.

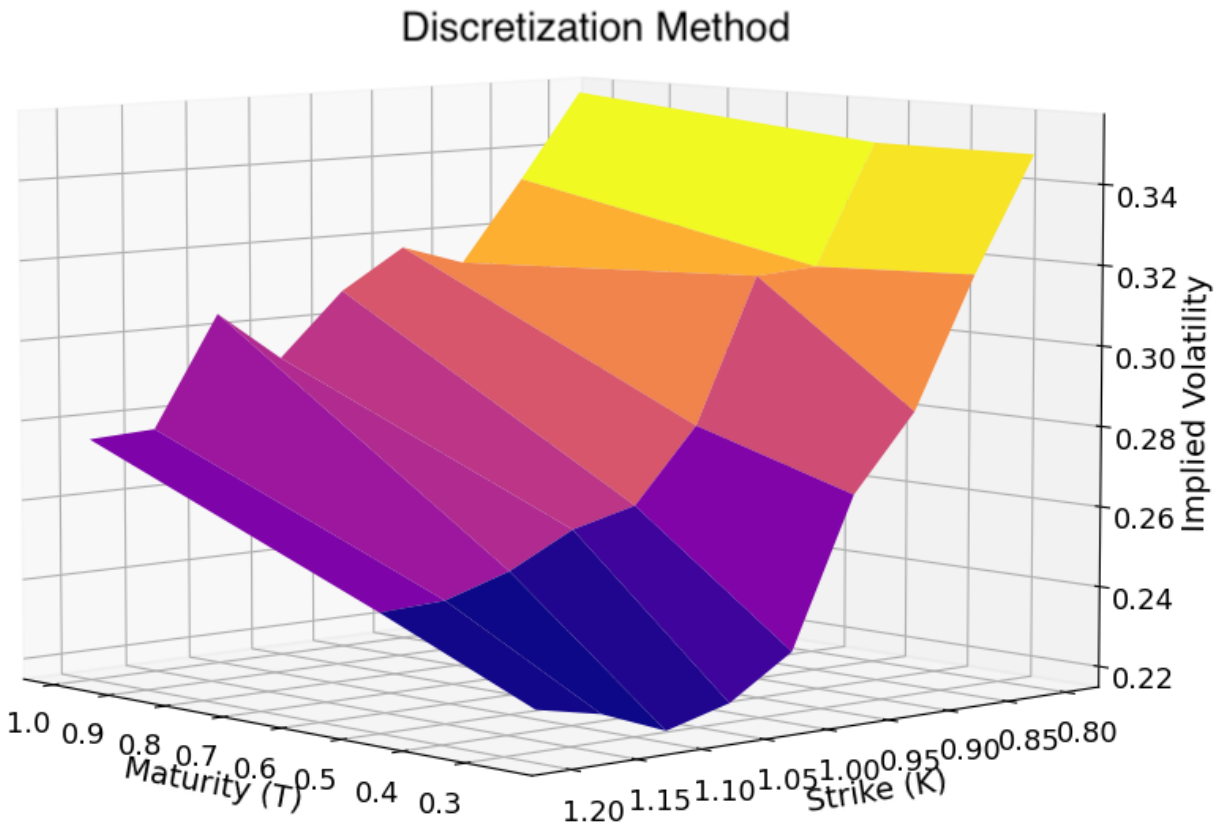


**Figure 3:** Implied volatility surface for a collection of strike prices and maturities. The surface has the expected structure of an increased implied volatility for greater maturities, and smaller strike prices.

It can be seen from the plot that the implied volatility surface is does not have smooth transitions between strike prices and maturities as would be expected due to the accuracy of the discretization method as described previously. This same effect was also seen in the fixed maturity implied volatility smiles. However, the overall implied volatility surface is similar to what would be expected, with the strike price having less of an effect on the implied volatility for greater maturities. The discretization method shows that there is room for improvement in the numerical accuracy of the implied volatility calculations, and the use of the mixing method will hopefully remedy some of the discretization method shortcomings.

### 4.1.2 Mixing Method

The use of a partial analytical solution in the mixing method should in principle improve the accuracy of the implied volatility calculations, the implied volatility surface and smiles will be investigated to see if this is true. The same implied volatility plots as were used in the discretization method section will be used for the mixing method so that the differences between the results can be directly compared. The plot of the implied volatility smile for various strike prices at a fixed maturity of $T = \frac{1}{4}$ is given below.

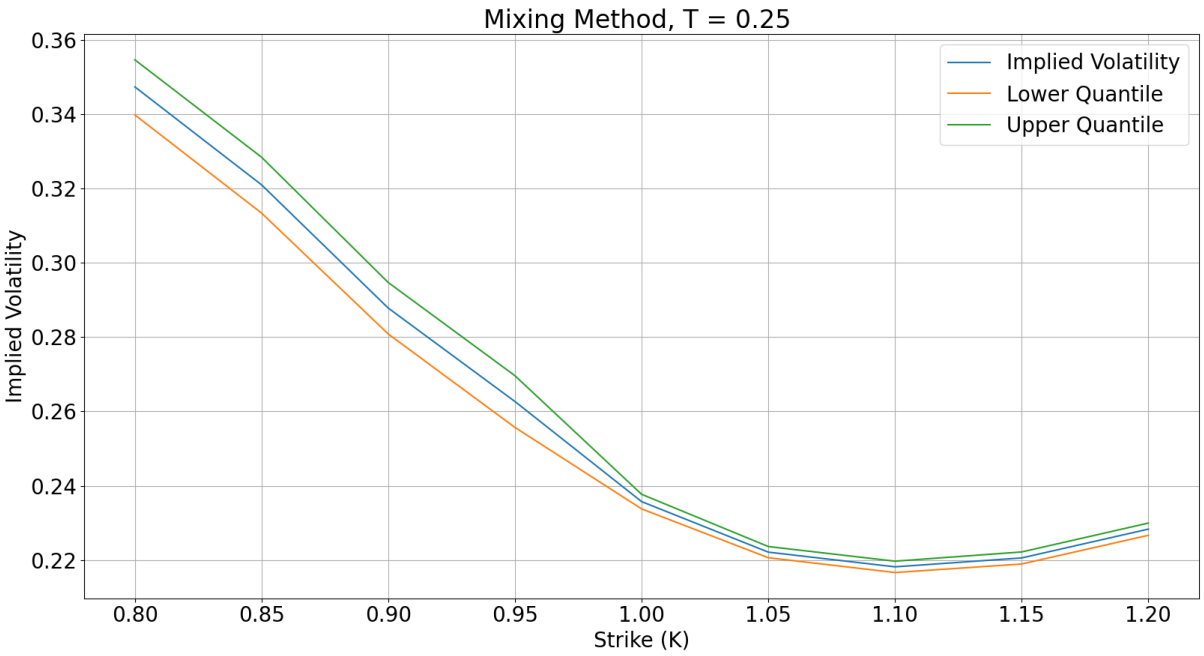


**Figure 4:** Changes to implied volatility as a function of the strike price for fixed maturity $T = \frac{1}{4}$. The volatility smile appears more so as a smirk, with the implied volatility being positively skewed for the domain of strikes where it has been calculated.

The confidence interval for the above plot starts with a band size of about, 0.01 but as the implied volatility decreases, the band size of the confidence interval decreases as well until it is well under its original size of 0.01. Comparing this to the same plot using the discretization method, it can be seen that the mixing method has a much more narrow confidence interval even at large implied volatilities which become even more narrow at lower implied volatilities. This is already an indication that the mixing method is performing better than the discretization method. Additionally, the volatility smile for the mixing method has a shape that is more similar to the expected parabolic curve shape than the discretization method. Overall, the range of the implied volatility for the mixing method is similar to the discretization method, but the shape of the curve is more accurate and the confidence interval is more narrow for the mixing method.

The plot of the implied volatility at a fixed maturity of $T = 1$ is now investigated for the mixing method.

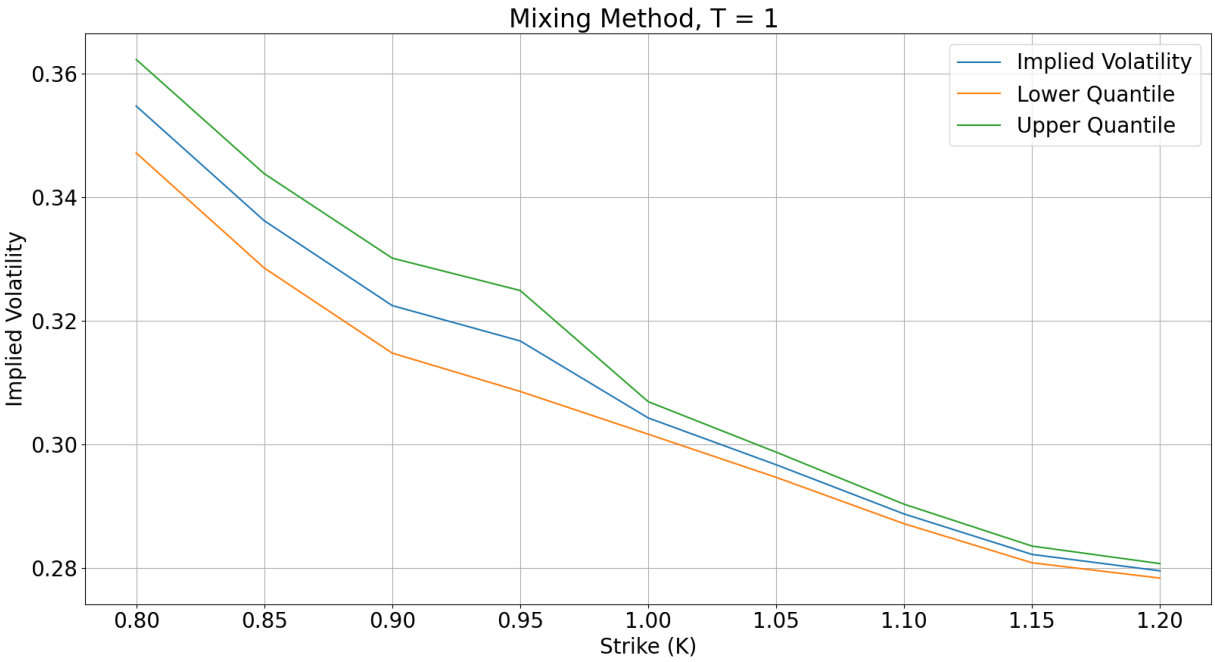


**Figure 5:** Changes to implied volatility as a function of the strike price for fixed maturity $T = 1$. The volatility smile appears more so as a decreasing trend rather than a smirk or smile, with the implied volatility being positively skewed for the domain of strikes where it has been calculated.

A similar trend of decreased confidence interval band size as implied volatility decreases as seen in the $T = \frac{1}{4}$ maturity plot is seen in the above $T = 1$ plot as well. Comparing to the same $T = 1$ plot for the discretization method, it can be seen that the mixing method does not have certain strike prices where the implied volatility increases when it should be decreasing, as is seen in the discretization method plot. Another indicator that the mixing method is more accurate. The overall expected parabolic structure is also more apparent in the mixing method plot. The range of implied volatilites for the discretization method and mixing method is similar.

The complete implied volatility surface for the collection of maturities and strike prices is now investigated for the mixing method.

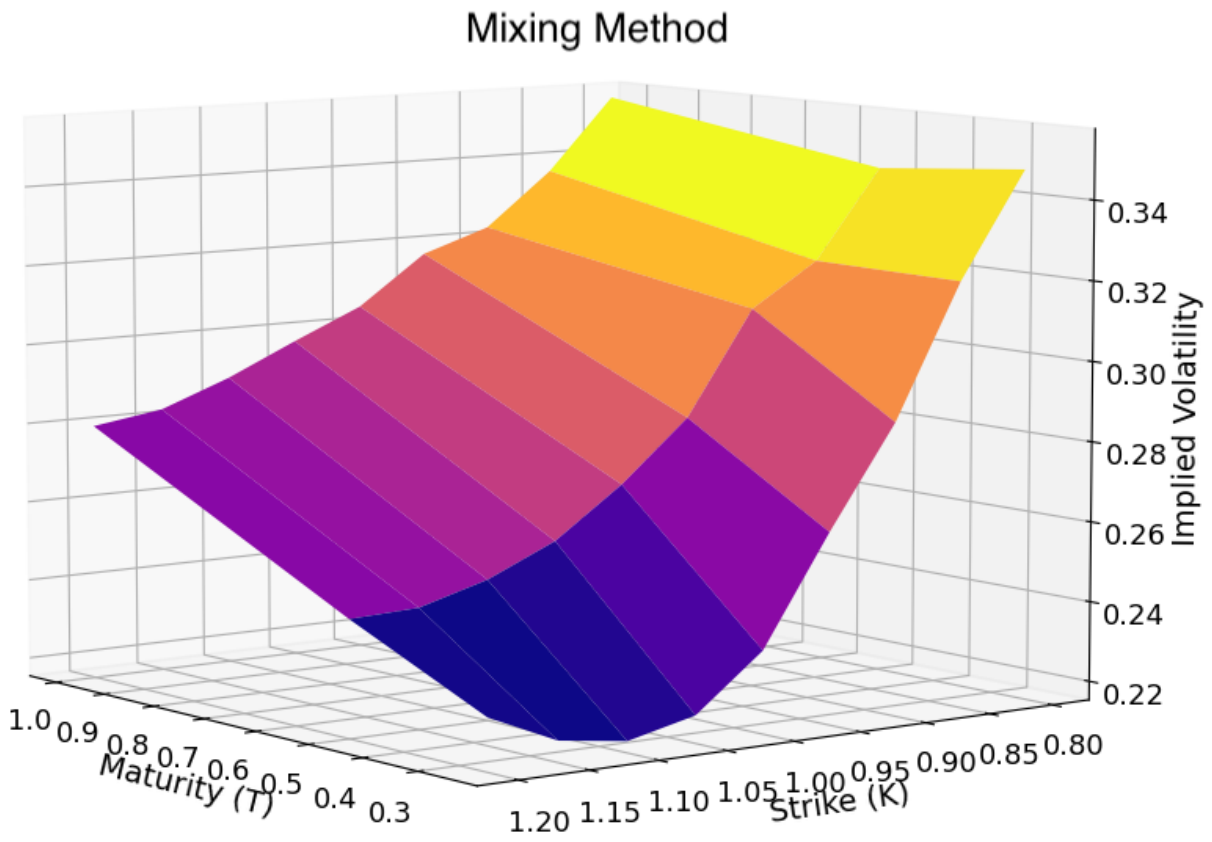


**Figure 6:** Implied volatility surface for a collection of strike prices and maturities. The surface has the expected structure of an increased implied volatility for greater maturities, and smaller strike prices.

The implied volatility surface has the same overall correct trends as is expected and was seen and described for the discretization implied volatility surface. However, for the mixing method, the overall shape is much smoother and resemble the expected shape of an implied volatility surface more closely. With less off trend variations in the implied volatility surface in the mixing method, it is much easier to see how the strike and maturity affect the implied volatility for the Heston model. Comparing all the implied volatility plots between the discretization method and mixing method, the mixing method shows more accurate results for all of them, indicating that it is the superior numerical method for simulating implied volatilities.

## 4.2 Contingent Claim Valuation

The valuation of a contingent claim paying $\int_0^T v_s ds$ at maturity $T$ is calculated analytically and numerically using the Milstein method. This is done for a collection of different maturity times and the results from the calculations are given in the table below.

Payoff: $\int_0^T v_s ds$

| Maturity ($T$) | Analytical Value | Simulated Value |
|---|---|---|
| 0.1 | 0.0056 | 0.0057 |
| 0.2 | 0.0139 | 0.0138 |
| 0.3 | 0.0243 | 0.0248 |
| 0.4 | 0.0360 | 0.0365 |
| 0.5 | 0.0489 | 0.0494 |
| 0.6 | 0.0627 | 0.0635 |
| 0.7 | 0.0768 | 0.0757 |
| 0.8 | 0.0916 | 0.0903 |
| 0.9 | 0.1066 | 0.1058 |
| 1.0 | 0.1219 | 0.1201 |

**Table 1:** Table of valuation for a contingent claiming paying $\int_0^T v_s ds$ at maturity. Analytical and simulated claim valuations are compared for a variety of claim maturities.

The tables are not very informative, and a plot comparing the value of the contingent claim at different maturities for the simulated and analytical value can be constructed.

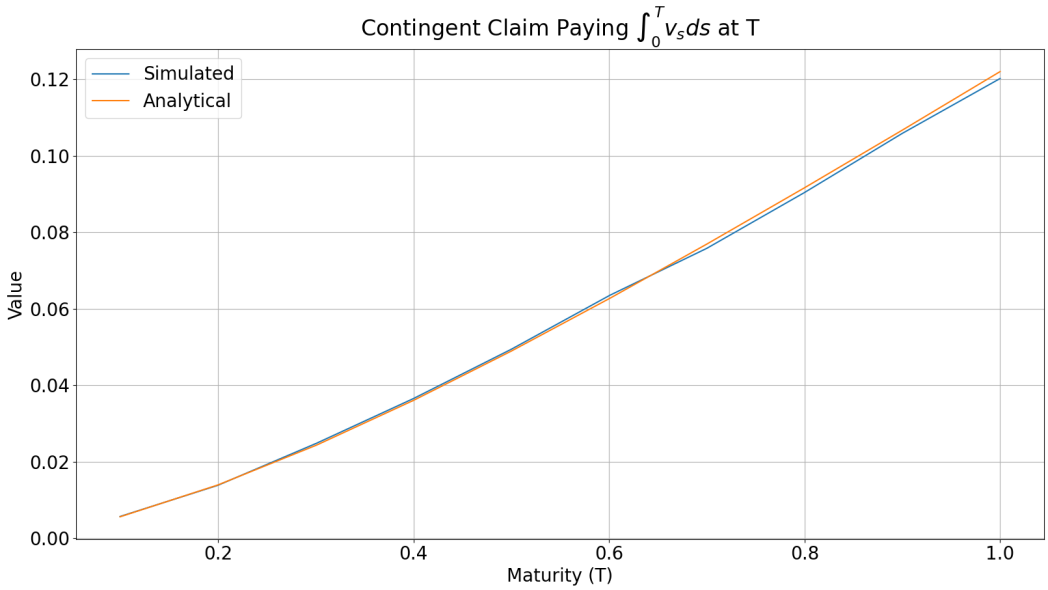


**Figure 7:** Analytical and simulated value of a contingent claim paying $\int_0^T v_s ds$ at maturity for a variety of different maturities. The simulated and analytical values take on very similar values.

It can be seen that the valuation between the analytical and numerical method differ slightly for every maturity. This is not unexpected as a finite number of time step intervals are used for the numerical integration and a finite number of simulations are used for the Monte Carlo simulation. As well, the Milstein method for the volatility is not perfectly accurate either as the confidence intervals are of finite extent, as was seen in the implied volatility smiles for the mixing method.

The valuation of a contingent claim paying $\int_0^T v_s^2 ds$ at maturity $T$ is calculated analytically and numerically using the Milstein method. This is done for a collection of different maturity times and the results from the calculations are given in the table below.

| Payoff: $\int_0^T v_s^2 ds$ | | |
|---|---|---|
| Maturity ($T$) | Analytical Value | Simulated Value |
| 0.1 | 0.0008 | 0.0008 |
| 0.2 | 0.0029 | 0.0029 |
| 0.3 | 0.0064 | 0.0068 |
| 0.4 | 0.0110 | 0.0112 |
| 0.5 | 0.0165 | 0.0165 |
| 0.6 | 0.0228 | 0.0227 |
| 0.7 | 0.0296 | 0.0291 |
| 0.8 | 0.0369 | 0.0355 |
| 0.9 | 0.0444 | 0.0429 |
| 1.0 | 0.0523 | 0.0499 |

**Table 2:** Table of valuation for a contingent claiming paying $\int_0^T v_s^2 ds$ at maturity. Analytical and simulated claim valuations are compared for a variety of claim maturities.

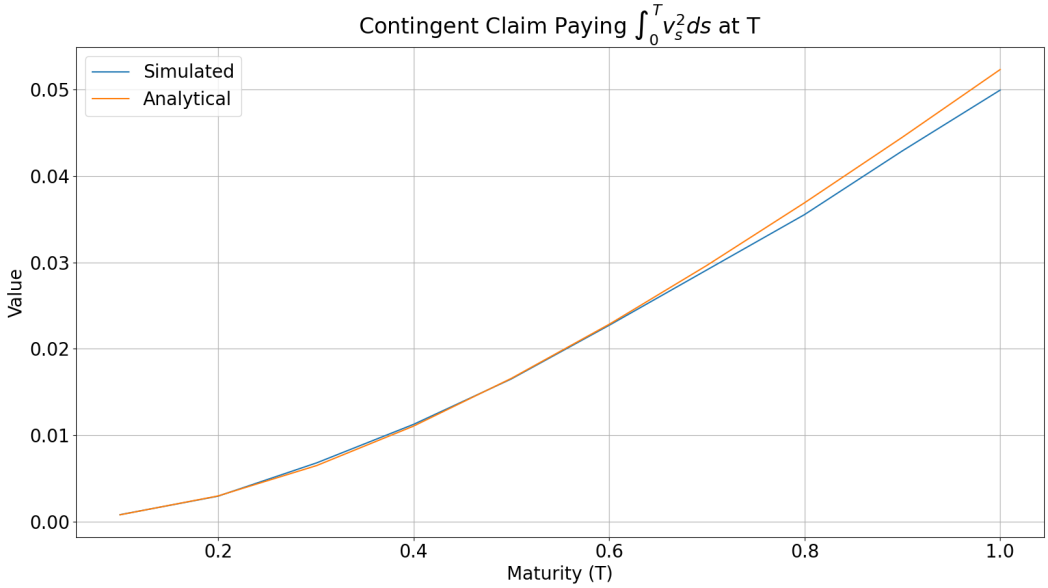


**Figure 8:** Analytical and simulated value of a contingent claim paying $\int_0^T v_s^2 ds$ at maturity for a variety of different maturities. The simulated and analytical values take on very similar values.

As seen for the other contingent claim, the valuation for the analytical and simulated values slightly differ. The same reasoning for the differences in valuations between the two methods from the previous contingent claim can be used for this contingent claim.

It has been successfully verified that the analytical and numerical valuations of the contingent claim agree with each other, and so we can be confident that the correct results will be implemented in the control variate method.

## 4.3 Implied Volatilities from Control Variate Simulations

A collection of control variates were implemented to improve the simulation accuracy for implied volatilities. These simulations were done on the Heston model and the Heston model with the volatility replaced with its expected value, making it a deterministic volatility model. The same numerical methods used in the discretization scheme were used for the control variates as well, the same collection of maturities and strike prices are also used. The four control variates exaimined are,

1. The option price using the deterministic variance path
2. A contingent claim paying $\int_0^T v_s ds$ at $T$
3. A contingent claim paying $\int_0^T v_s^2 ds$ at $T$
4. The stock price

To evaluate the performance of the models with the control variates in a straightforward manner, the absolute value of the difference between the lower quantile and average simulated value were averaged throughout the duration of the option, the same was done with the upper quantile and those two values were averaged, this was done for all three different maturities and those values were averaged to get a total average variation of the control variate models. This variation average can be compared to the simulations with different control variates to find the one that minimizes the variation and is therefore the best.

| Heston Model | |
|---|---|
| Control Variate | Variation Average |
| Deterministic Volatility Option | 0.0058 |
| $\int_0^T v_s ds$ | 0.0097 |
| $\int_0^T v_s^2 ds$ | 0.0099 |
| Stock | 0.0075 |
| All | 0.0042 |
| Mixing Method | 0.0064 |

**Table 3:** Table of variation average for different control variates in the Heston model.

| Deterministic Volatility Model | |
|---|---|
| Control Variate | Variation Average |
| Deterministic Volatility Option | $6.167 \times 10^{-16}$ |
| $\int_0^T v_s ds$ | 0.0093 |
| $\int_0^T v_s^2 ds$ | 0.0096 |
| Stock | 0.0074 |
| All | $1.233 \times 10^{-16}$ |

**Table 4:** Table of variation average for different control variates in the deterministic volatility model.

For both of the model types, the variate averages have the same trend, that is, the method with the contingent claim paying $\int_0^T v_s^2 ds$ as the control variate performs the worst, followed by the contingent claim paying $\int_0^T v_s ds$ as the control variate having slightly less average variation, the stock price as the control variate performed much better than the contingent claim control variates and the deterministic volatility option performed the best. For the deterministic volatility model, it is unsurprising that the deterministic volatility option control variate reduced the variation average to nearly zero as the option that the simulation is trying to value is the same as the control variate. The plots of the implied volatilities at constant maturity for a collection of different strike prices for the different control variate

methods is given in the appendix. These plots were not included in the main article as they are quite cluttered and should only be used for verification purposes. It is unsurprising that the deterministic volatility option is the best control variate, as it is very similar to the option price we are simulating in the Heston model, the exact same as the deterministic volatility model option valuation as well as similar to the Black-Scholes model option valuation, which is what we are trying to solve for to get the implied volatility. Whereas, the contingent claims over the integrals of the volatility do not appear directly in the option valuation expressions, even though they are related. The stock price appears directly in the option valuation expressions and so the trend of control variates seems logical. Using all the control variates unsurprisingly decreases the average variation, and therefore is the ensemble of all control variates is actually the best choice. The mixing method is also included for comparison with the all control variates method. It can be seen that all the control variates perform much better than the mixing method.

Plots of the implied volatilities for a collection of strikes at fixed maturity dates for the method using all control variates and the mixing method are given below.

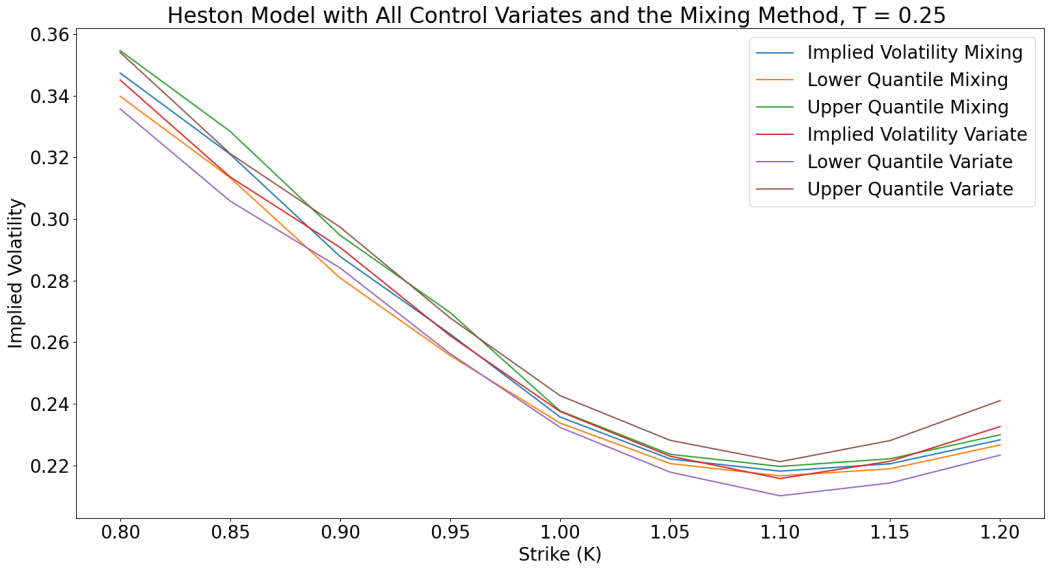


**Figure 9:** Changes to implied volatility as a function of the strike price for fixed maturity $T = \frac{1}{4}$ in the Heston model with all control variates and the mixing method.. The implied volatility and confident intervals are plotted.

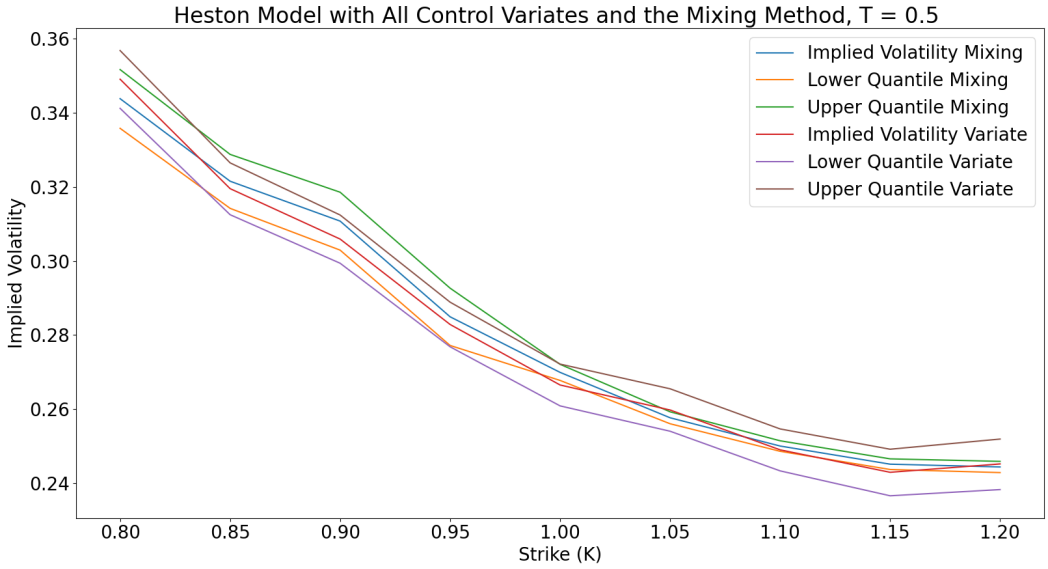


**Figure 10:** Changes to implied volatility as a function of the strike price for fixed maturity $T = \frac{1}{2}$ in the Heston model with all control variates and the mixing method.. The implied volatility and confident intervals are plotted.

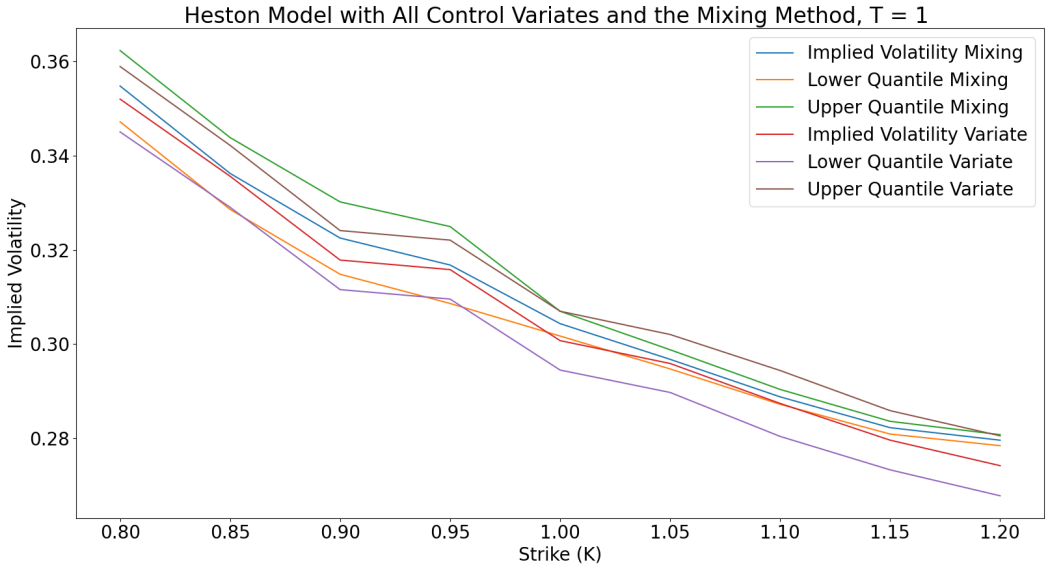


**Figure 11:** Changes to implied volatility as a function of the strike price for fixed maturity $T = 1$ in the Heston model with all control variates and the mixing method. The implied volatility and confident intervals are plotted.

The implied volatility plots for the all control variates method and the mixing method have slight variates between them, but the overall shape and structure is the same. It can be seen that all the control variates perform better than the mixing method. The reasoning for the improvement with the control variates is that the mixing method still requires the Milstein method to simulate the volatility. However, the contingent claim control variates are functions of the volatility and so will help to minimize the variations caused by the Milstein method. As well, the stock price and option price for the deterministic path are related to the option valuations needed to find the implied volatility and so minimize the variation in option valuation simulations. The combination of all these effects leads to a control variate method that outperforms a model that is almost entirely analytic, the mixing method. The minimization of variations ensures that the model is extremely close to the actual solution.

# 5 Conclusion

In this report, we investigated the Heston model through several aspects based on the model setup and mathematical derivations. First, we analyzed the implied volatility smiles with confidence intervals for both put and call options using different discretization techniques. Using Euler discretization by Monte Carlo simulation, the volatility smile does not have smooth transitions in the implied volatility between different strike prices, since the step size selection was quite coarse and that the discretization method can only act as an approximation. Using the mixing method, the volatility smile is more similar to the expected parabolic curve shape and it has a more narrow confidence interval even at large implied volatilities, indicating its better performance. We then studied the impact of different control variates to reduce the variance of a Monte Carlo simulation when having an analytic solution of a closely related model. For two target contingent claims, we confirmed that their analytical and numerical valuations agree with each other. Note that we also derived the expression of optimization parameter to minimize the model variance. We also simulated paths of the Heston model under the deterministic volatility and compared the best control variate between option, two contingent claims and stock using both Milstein method and Mixing method to compare their performance. We observed that for both of the model types, the variate averages have the same trend, that is, the method with both contingent claims perform the worst, the stock price as the control variate performed much better than the contingent claims and the deterministic volatility option performed the best. The mixing method is also included for comparison with the all control variates method. It can be seen that all the control variates perform much better than the mixing method than single discretization method.

# 6 Appendix: Discretization and Mixing Methods

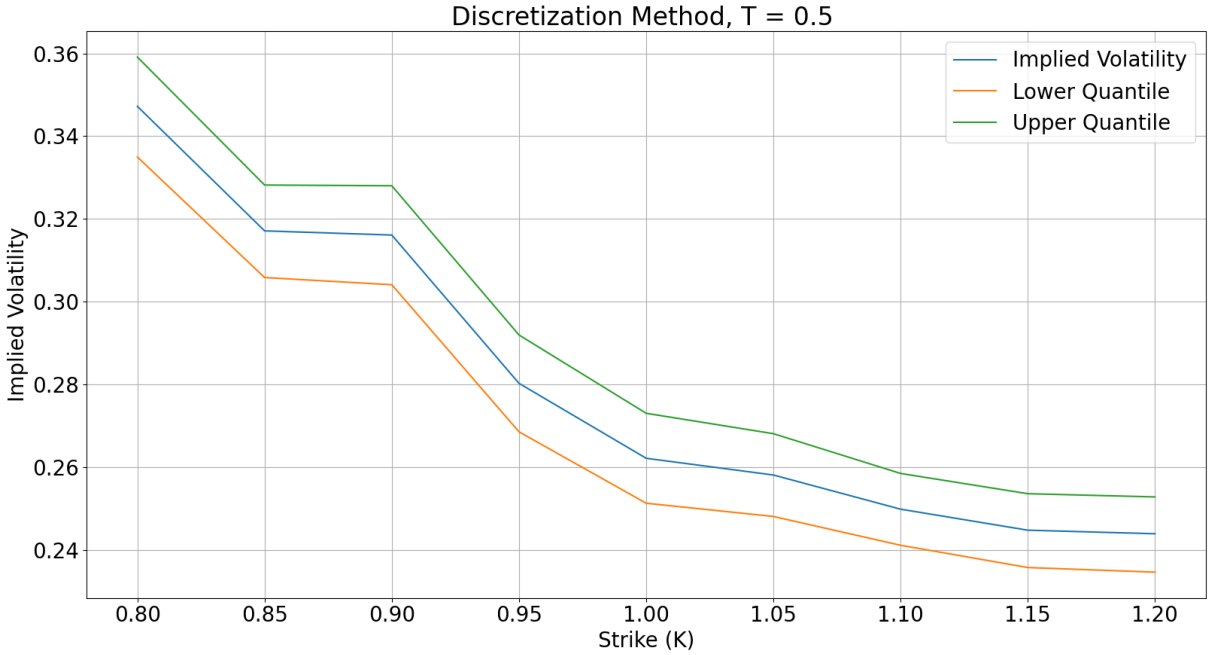


**Figure 12:** Changes to implied volatility as a function of the strike price for fixed maturity $T = \frac{1}{2}$. The volatility smile appears more so as a decreasing trend rather than a smirk or smile, with the implied volatility being positively skewed for the domain of strikes where it has been calculated.

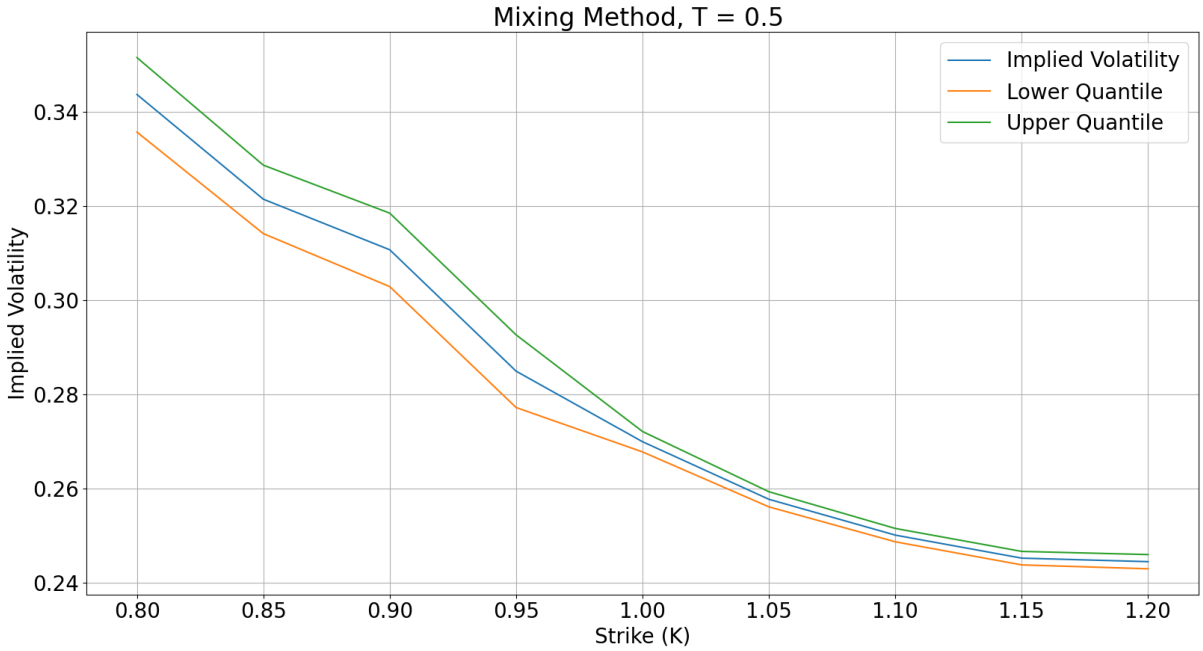


**Figure 13:** Changes to implied volatility as a function of the strike price for fixed maturity $T = \frac{1}{2}$. The volatility smile appears more so as a decreasing trend rather than a smirk or smile, with the implied volatility being positively skewed for the domain of strikes where it has been calculated.

# 7 Appendix: Control Variates

## 7.1 Claim Paying $\int_0^T v_s ds$

### 7.1.1 Heston Model

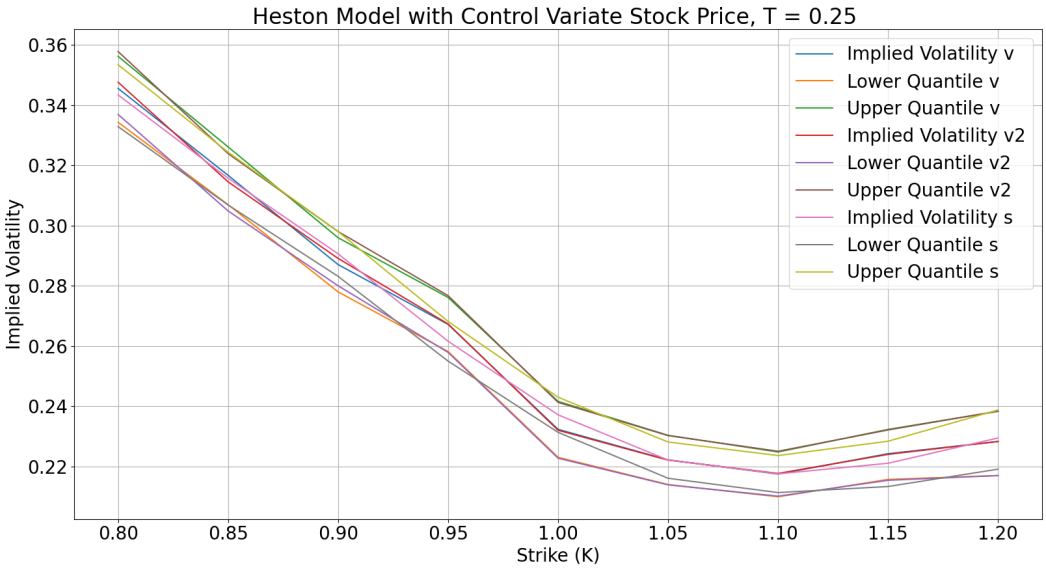


**Figure 14:** Changes to implied volatility as a function of the strike price for fixed maturity $T = \frac{1}{4}$ in the Heston model. The implied volatility and confident intervals are plotted for all control variate methods.

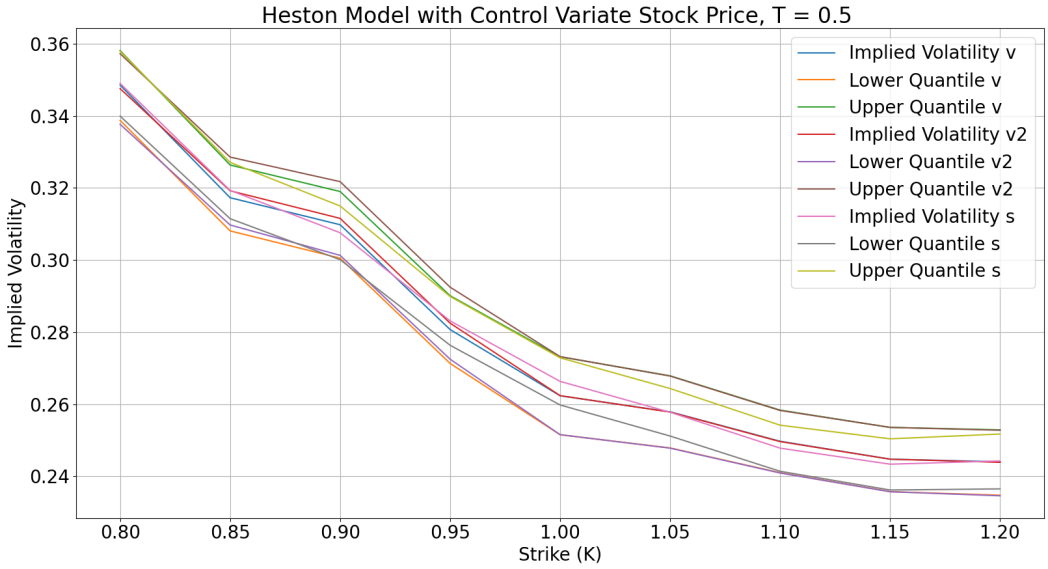


**Figure 15:** Changes to implied volatility as a function of the strike price for fixed maturity $T = \frac{1}{2}$ in the Heston model. The implied volatility and confident intervals are plotted for all control variate methods.

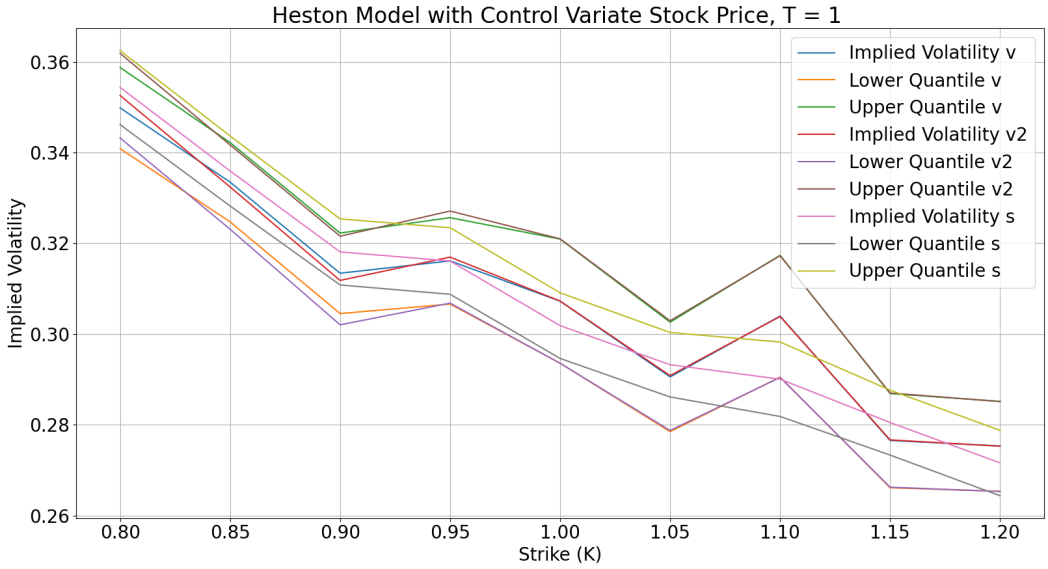


**Figure 16:** Changes to implied volatility as a function of the strike price for fixed maturity $T = 1$ in the Heston model. The implied volatility and confident intervals are plotted for all control variate methods.

### 7.1.2 Deterministic Volatility Model

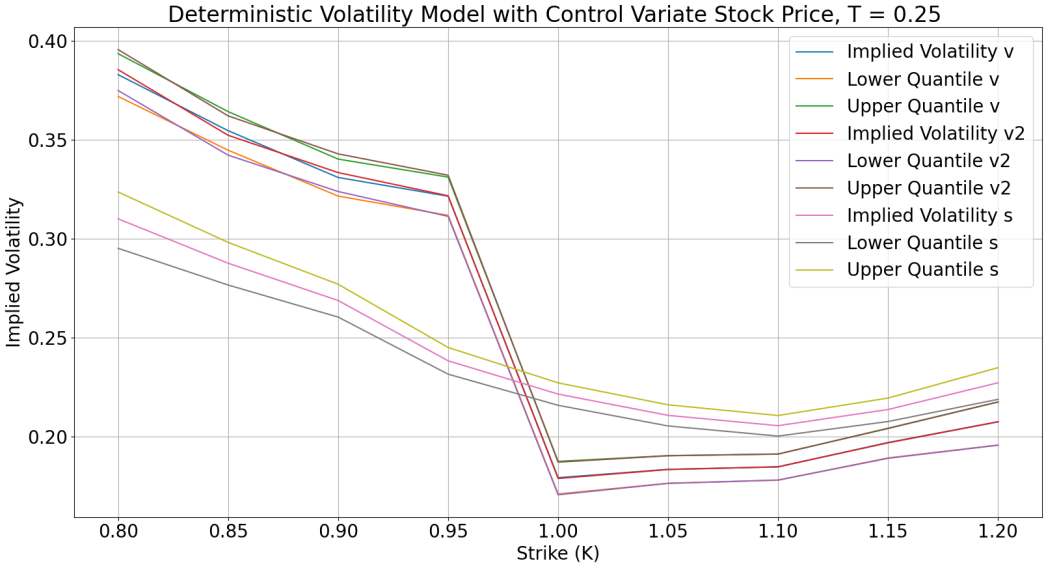


**Figure 17:** Changes to implied volatility as a function of the strike price for fixed maturity $T = \frac{1}{4}$ in the deterministic volatility model. The implied volatility and confident intervals are plotted for all control variate methods.

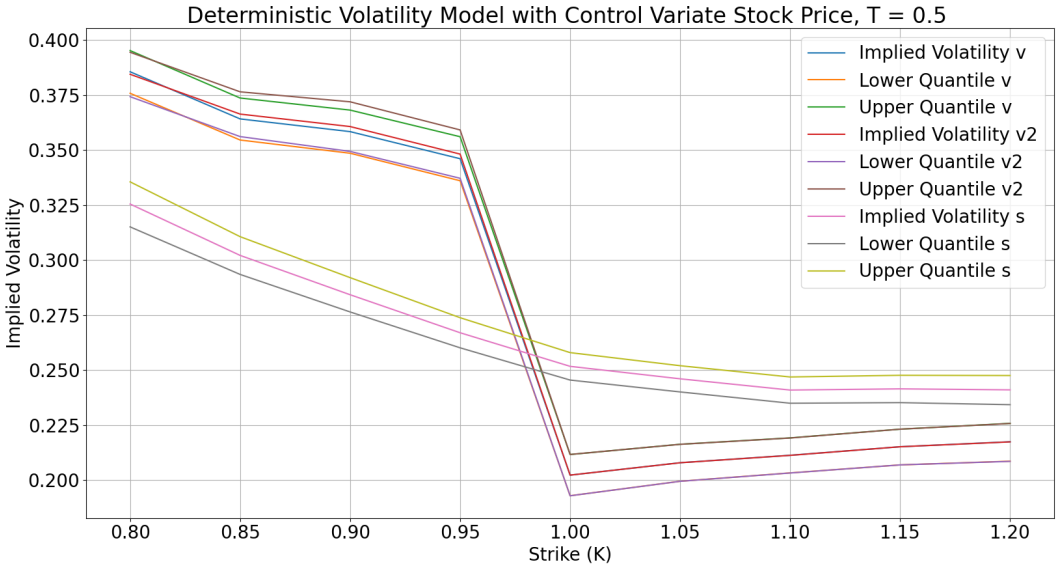


**Figure 18:** Changes to implied volatility as a function of the strike price for fixed maturity $T = \frac{1}{2}$ in the deterministic volatility model. The implied volatility and confident intervals are plotted for all control variate methods.

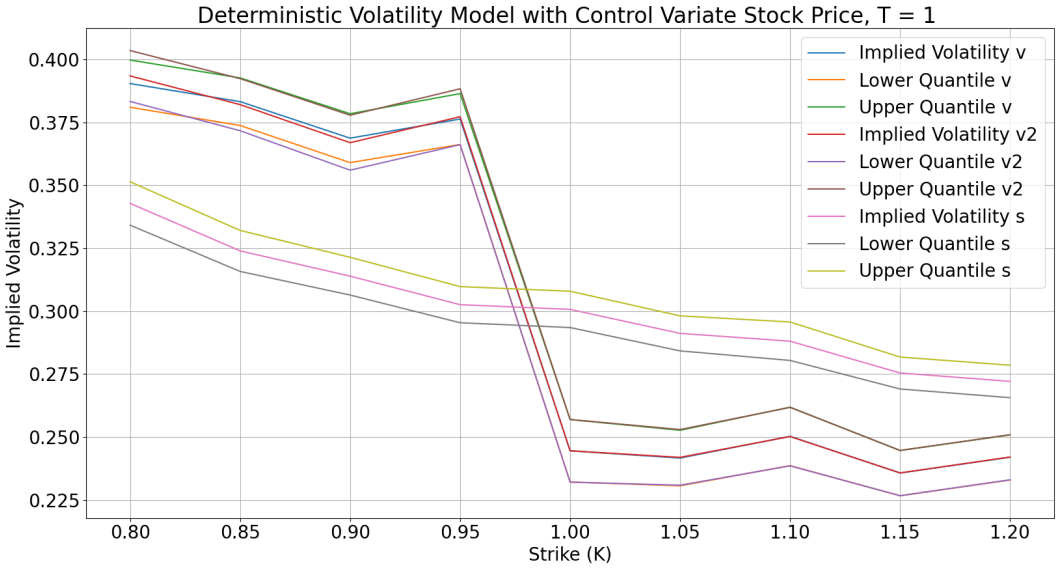


**Figure 19:** Changes to implied volatility as a function of the strike price for fixed maturity $T = 1$ in the deterministic volatility model. The implied volatility and confident intervals are plotted for all control variate methods.